MOLECULAR SIEVES

1. Introduction

In the broadest sense, any materia l that can exclude molecular species by size can be considered a molecular sieve. However, in this article the term molecular sieve is restricted to inorganic materials that possess uniform pores with diameters in either the micro- (<2 nm), meso- (2–50 nm), or macro (50–200 nm) size range. The most technologically important molecular sieves are zeolites, ie, crystalline silicate or aluminosilicate framework structures with channels of diameters <1.2 nm (1). Several of these topologies, with boron, gallium, or iron replacing aluminum, or germanium replacing silicon, have also been prepared. The chemical composition of microporous framework structures has been expanded considerably with the substitution of phosphorus for silicon and new families of aluminophosphate (2) and silicoaluminophosphate (3) structures have been synthesized in the laboratory. Some of these new frameworks have zeolite analogues, whereas others are unique. The addition of elements such as Mg, Ti, Mn, Co, Fe, or Zn into these structures has made it possible to generate

metalloaluminophosphates (4), metallosilicoaluminophosphates (5), etc. Microporous sulfide-based framework structures are also possible (6).

Considerable synthesis effort has been devoted to developing frameworks with larger pore diameters within the microporous range; the largest synthesized are AlPO-8 (7), CIT-5 (8), UTD-1 (9), OSB-1 (10), SSZ-53, SSZ-59 (14-membered ring) (10), VPI-5, ECR-34 (18-MR) (11), and cloverite (20-MR) (12), which have pore diameters within the 0.7–1.3-nm range. Cacoxenite, a natural ferroaluminophosphate, has been structurally characterized as having ~1.4-nm channels that approach the mesoporous size range (13). A new family of mesoporous molecular sieves designated M41S has been discovered (14). Although not framework structures like zeolites, silicate and aluminosilicate M41S materials possess very uniform mesopores. The regime of pore sizes for the ordered mesoporous materials have been expanded to ~50 nm by the synthesis of SBA-15 (15). Other chemical compositions are possible (16) and this area has afforded a myriad of materials with potential as high surface area supports for catalysis and separation applications. Recently materials with three-dimensionally ordered macroporous have been generated in various chemical compositions (17).

The technological applications of molecular sieves are as varied as their chemical makeup. Heterogeneous catalysis and adsorption processes make extensive use of molecular sieves. The utility of the latter materials lies in their microstructures, which allow access to large internal surfaces, and cavities that enhance catalytic activity and adsorptive capacity.

2. Zeolites

Molecular-sieve zeolites of the most important aluminosilicate variety can be represented by the chemical formula $M_{2/n}O{\cdot}Al_2O_3{\cdot}ySiO_2{\cdot}wH_2O$, where y is 2 or greater, M is the charge balancing cation, such as sodium, potassium, magnesium, and calcium, n is the cation valence, and w represents the moles of water contained in the zeolitic voids. The zeolite framework is made up of SiO_4 tetrahedra linked together by sharing of oxygen ions. Substitution of Al for Si generates a charge imbalance, necessitating the inclusion of a cation. The structures contain channels or interconnected voids that are occupied by the cations and water molecules. The water may be removed reversibly, generally by the application of heat, which leaves intact the crystalline host structure permeated with micropores that may account for >50% of the microcrystal's volume. In some zeolites, dehydration may produce some perturbation of the structure, such as cation movement, and some degree of framework distortion.

Zeolites were first recognized as a new type of mineral in 1756 by the Swedish mineralogist A. F. Cronstedt (18). The word "zeolite" was derived from two Greek words, ζειν and λιθο, meaning to boil and a stone. More than 200 synthetic zeolite types and 50 natural zeolites are known. The nomenclature of zeolite minerals follows established procedures. Both synthetic and natural zeolites of different topologies are given three-letter codes by the International Zeolite Association (19).

Zeolite minerals are formed over much of the earth's surface, including the sea bottom (20). However, with a few notable exceptions, they are exceedingly

Table 1. **Zeolite Compositions**

Zeolite	CAS Registry number	Typical formula
		Natural
chabazite	[12251-32-0]	$Ca_2[(AlO_2)_4(SiO_2)_8]\cdot 13H_2O$
mordenite	[12173-98-7]	$Na_8[(AlO_2)_8(SiO_2)_{40}]\cdot 24H_2O$
erionite	[12150-42-8]	$(Ca, Mg, Na_2, K_2)_{4.5}[(AlO_2)_9(SiO_2)_{27}]\cdot 27H_2O$
faujasite	[12173-28-3]	$(Ca, Mg, Na_2, K_2)_{29.5}[(AlO_2)_{59}(SiO_2)_{133}]\cdot 235H_2O$
clinoptilolite		$Na_6[(AlO_2)_6(SiO_2)_{30}]\cdot 24H_2O$
phillipsite	[12321-85-6]	$(0.5Ca, Na, K)_3[(AlO_2)_3(SiO_2)_5]\cdot 6H_2O$
		Synthetic
zeolite A		$Na_{12}[(AlO_2)_{12}(SiO_2)_{12}]\cdot 27H_2O$
zeolite X	[68989-23-1]	$Na_{86}[(AlO_2)_{86}(SiO_2)_{106}]\cdot 264H_2O$
zeolite Y		$Na_{56}[(AlO_2)_{56}(SiO_2)_{136}]\cdot 250H_2O$
zeolite L		$K_9[(AlO_2)_9(SiO_2)_{27}]\cdot 22H_2O$
zeolite omega		$Na_{6.8}TMA_{1.6}[(AlO_2)_8(SiO_2)_{28}]\cdot 21H_2O$[a]
ZSM-5	[58339-99-4]	$(Na, TPA)_3[(AlO_2)_3(SiO_2)_{93}]\cdot 16H_2O$[b]

[a]TMA = tetramethylammonium.
[b]TPA = tetrapropylammonium.

rare. Until the early 1960s, zeolite minerals were thought to occur mainly in cavities of basaltic and volcanic rocks. Since then, several zeolite minerals formed by the natural alteration of volcanic ash in alkaline environments over long periods of time, eg, in Cenozoic lakes, such as the alkaline lake beds of the western United States, have been identified through the use of X-ray diffraction techniques. The more common topological types that have been identified there include analcime (ANA), clinoptilolite (HEU), mordenite (MOR), chabazite (CHA), erionite (ERI), and phillipsite (PHI) (Table 1). Owing to the hydrolysis of the alkaline constituents of the volcanic ash, the water in these lakes became salty and alkaline (pH up to 9.5), which resulted in the crystallization of zeolites from this deposit. The resulting zeolites were produced as readily accessible flat-lying beds. Of the ~50 known zeolite minerals, chabazite, erionite, mordenite, and clinoptilolite occur in sufficient quantity and purity to allow their use as commercial products.

A less ancient zeolite formation process occurred through the percolation of surface water through appropriate sediments. The city of Naples, Italy, is underlain by a zeolitic deposit some 200 km^2 (77 mi^2) in area which is only 5–10 thousand years old. Two large-pore zeolites recently discovered in Oregon, boggsite (BOG) and tschernichite, the latter a natural version of zeolite beta, were formed by percolation of rainwater through basaltic rock (21). The locality Jurassic Ferrar dolerites of Mt. Adamson in North Victoria Land, Antartica has recently revealed to be extraordinarily rich in zeolites. Besides finding the rare minerals boggsite and tschernichite, other novel minerals have been discovered such as gottardiite a natural version of NU-87 (22), terranovaite a new zeolite topology (23) and most importantly mutinaite the natural version of ZSM-5 (24).

In general, high grade zeolite ore is mined and then processed by crushing, drying, powdering, and screening. Depending on its intended use, it may then be

chemically modified, eg, by ion exchange, acid extraction, etc, and calcined at 350–550°C.

3. Structure

Of the ~136 known framework types 75 are silicates, ~46 are phosphate based and 25 can occur as both. Only ~60 of the structurally characterized zeolites are found in nature so far. Understanding the complexities of zeolite structures is made easier by recognizing three important structural keys: the basic arrangement of the individual structural units in space, which defines the framework topology; the location of the charge-balancing cations; and the channel-filling material, such as water or an organic template, which is incorporated as the zeolite is formed. After the channel-filling material is removed, the void space can be used for the adsorption of gases, liquids, salts, elements, metal complexes, etc. In turn, this void-filling property makes zeolites commercially useful in ion exchange, catalysis, etc. The current concepts of zeolite structure were developed by Pauling in 1930 (25). Modern characterization tools such as X-ray, electron and neutron diffraction, infrared and Raman spectroscopies, nuclear magnetic resonance (nmr), and electron microscopy have provided a very detailed description of many structures. Computer-based structure determination techniques have been developed, and computer-aided tools, such as Fourier transform infrared (FTIR) and ultraviolet–visible (uv–vis), are being used for characterization of zeolites.

There are two types of structures: one provides an internal pore system comprising interconnected cage-like voids; the second provides a system of uniform channels which, in some instances, are one-dimensional (1D) and in others intersect with similar channels to produce two (2D)- or three-dimensional (3D) channel systems. The preferred type has two- or three-dimensional channel systems to provide rapid intracrystalline diffusion in adsorption and catalytic applications.

In most zeolite structures, the primary structural units, tetrahedra, are assembled into secondary building units, which may be simple polyhedra such as cubes, hexagonal prisms, or truncated octahedra. The final framework structure consists of assemblages of the secondary units. These assemblages of secondary units are a convenient means of grouping frameworks by similar units, but should not necessarily be used as a model for zeolite nucleation processes. Models of the structures are often constructed of skeletal tetrahedra. Space-filling models demonstrating the preponderance of oxygen ions are more realistic, but more difficult to construct (Fig. 1).

3.1. Zeolite Minerals. Crystal structures of zeolite minerals are illustrated by the zeolites chabazite and mordenite. The structure of chabazite is hexagonal and the framework consists of double six-membered rings of (Si, Al)O_4 tetrahedra arranged in parallel layers in an AABBCC sequence. These tetrahedra are cross-linked by four-membered rings, as shown in Figure 2, resulting in cavities, 0.67×1.0 nm, each of which is entered by elliptical apertures 0.44×0.31 nm. Exchangeable metal ions, such as calcium, occupy positions within or near the double six-membered rings. The mineral mordenite is more complex, as illustrated in Figure 3, and provides for a one-dimensional channel

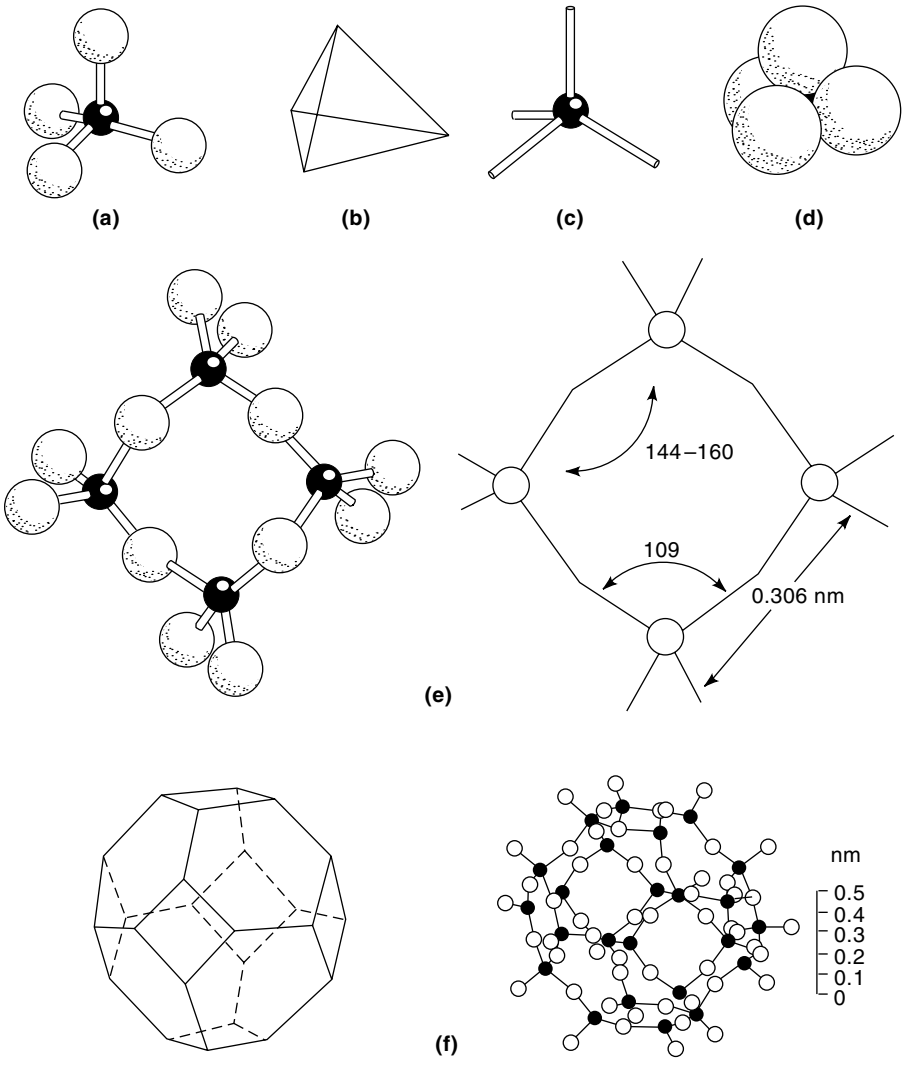

Fig. 1. Methods for representing SiO_4 and AlO_4 tetrahedra by means of (**a**) ball-and-stick model, (**b**) solid tetrahedron, (**c**) skeletal tetrahedron, and (**d**) space-filling of packed spheres (1). (**e**) Linking of four tetrahedra in a four-membered ring. (**f**) Secondary building unit called truncated octahedron as represented by a solid model, left, and a ball-and-stick model, right.

of $\sim 0.6 \times 0.7$ nm. The framework itself is built from chains of five-membered rings that are cross-linked. The mineral does not exhibit adsorption properties commensurate with the channel size, apparently because of occluded material.

Several properties of zeolite minerals were studied, including adsorption and ion exchange. This led to the preparation of amorphous aluminosilicate ion exchangers for use in water softening. Studies of the gas-adsorption properties of dehydrated natural zeolite crystals in the 1920s led to the discovery of their molecular-sieve behavior (26). As microporous solids with uniform pore

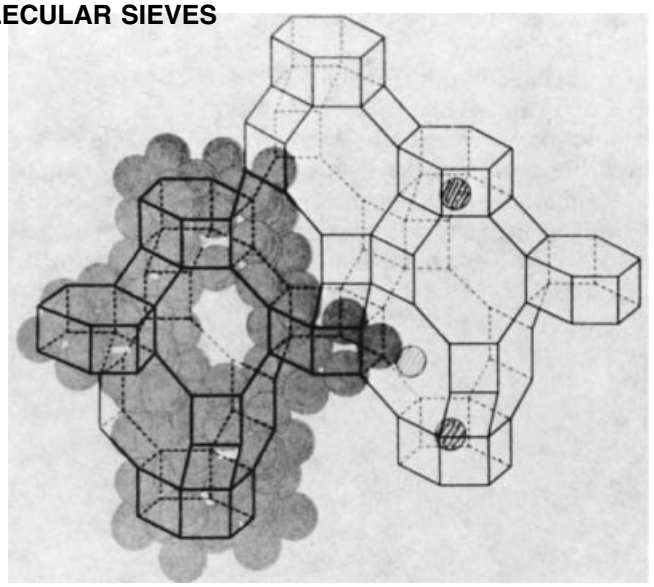

Fig. 2. Structure of the mineral zeolite chabazite is depicted by packing model, left, and skeletal model, right. The silicon and aluminum atoms lie at the corners of the framework depicted by solid lines. In this figure, and Figure 1, the solid lines do not depict chemical bonds. Oxygen atoms lie near the midpoint of the lines connecting framework corners. Cation sites are shown in three different locations referred to as sites I, II, and III. (Courtesy of Scientific American.)

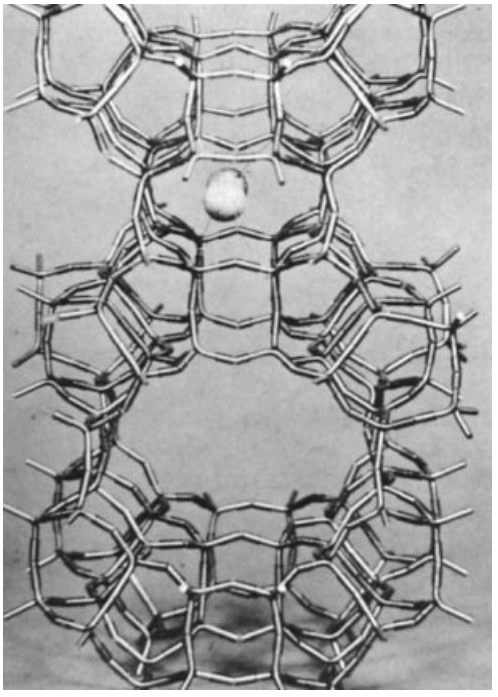

Fig. 3. Model of the crystal structure of the mineral mordenite showing the main channel formed by 12-membered ring and small channels that contain some of the sodium cations. Synthetic types of mordenite exhibit the adsorption behavior of a 12-membered ring, whereas the mineral does not, probably owing to channel blocking.

sizes that range from 0.3 to 1.8 nm, these materials can selectively adsorb or reject molecules based on their molecular size. This effect, with obvious commercial potential leading to novel processes for separation of materials, inspired attempts to duplicate the natural materials by synthesis.

3.2. Synthetic Zeolites. Many new crystalline zeolites have been synthesized and several fulfill important functions in the chemical and petroleum industries and in consumer products such as detergents. The structural formula of a zeolite is based on the crystal unit cell, the smallest unit of structure, represented by $M_{x/n}[(AlO_2)_x(SiO_2)_y]\cdot wH_2O$, where n is the valence of cation M, w is the number of water molecules per unit cell, x and y are, respectively, the number of AlO_4 and SiO_4 tetrahedra per unit cell, and y/x usually has values of 1–5. Examples of important synthetic zeolites are shown in Table 1. These include zeolites A, X, Y, and Zeolon, a synthetic form of mordenite. Subsequently synthesized high silica zeolites include ZSM-5 (27) and ZSM-11, in which y/x is 10->5000 and molecular sieves consisting essentially of silica have been prepared; the first one of this type, a high silica form of ZSM-5, was named silicalite (28).

The secondary structure unit in zeolites A, X, and Y is the truncated octahedron shown in Figure 1 **f**. These polyhedral units are linked in 3D space through the four- or six-membered rings. The former linkage produces the zeolite A structure and the latter the topology of zeolites X and Y and of the mineral faujasite. In zeolite A, the internal cavity is 1.1 nm in diameter and is entered by six circular apertures 0.41 nm in size. The interlinked cavities form 3D, undulated channels with a 0.41 nm minimum diameter. The sodium ions are located in the six-membered rings and near the eight-membered rings (29). The faujasite-type structure consists of a tetrahedral arrangement of the truncated octahedra by joining of the six-membered rings. The resulting cages are 1.3 nm in size, and each is entered by a 12-membered channel of 0.74 nm in diameter. This is one of the larger pore sizes in zeolites. Figure 4 illustrates several types of cation positions; some lie within the smaller polyhedra and some are exposed on the internal surface (1). A slightly different stacking of the truncated cubooctahedrahexagonal prisms combination results in the hexagonal structure of EMC-2 (EMT) having one straight channel formed by 12-membered rings of 0.73 nm crystallographic diameter (19). These channels are connected in the α-direction by 12-membered rings of 0.74×0.65 nm in size. The similarity of these two structures permits intergrowth of the different unit cells within the same crystal, eg, ZSM-20. The structure of ZSM-5 (Fig. 5) contains a high concentration of five-membered rings and provides two sets of intersecting channels with pore sizes of 0.56×0.53 and 0.55×0.51 nm (28).

Many of the novel silica-based zeolite structures are derived from the use of organocations as guest molecules in the crystallization product. The organocations effectively stabilize the void regions within the inorganic structure and have been referred to as "template" molecules or "structure directing agents." The size and shape of the guest molecule often correlate well with the void dimensions within the host, however there are still aspects of phase selectivity in zeolite synthesis that are kinetically controlled. Research in modeling the guest–host interactions and from the empirical learning from four decades of zeolite synthesis strategies, a myriad of large pore silica zeolites have been discovered and some representative materials are CIT-5 (8), UTD-1 (9), SSZ-48 (30),

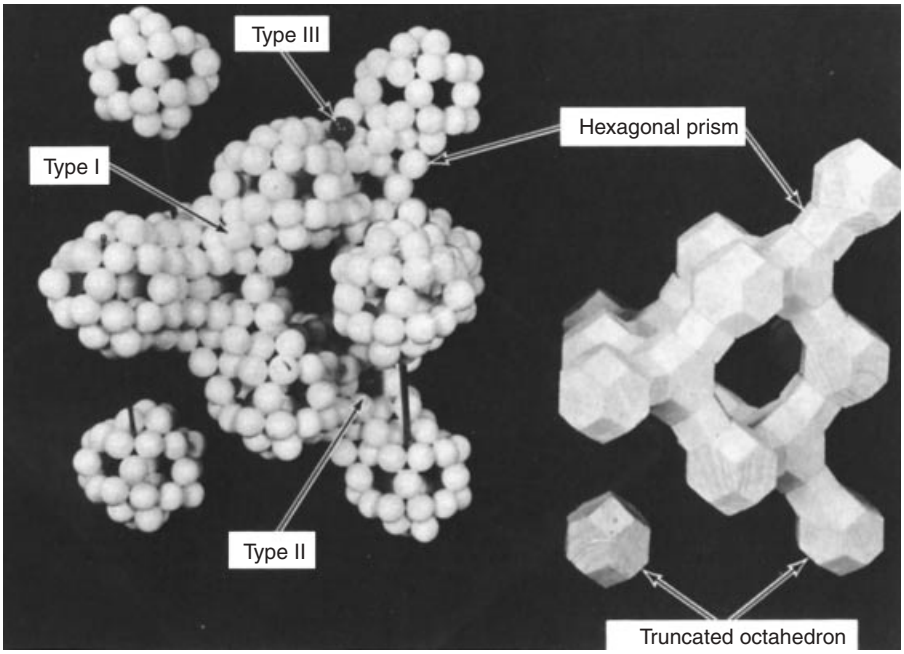

Fig. 4. Model of the crystal structure of zeolites X, Y, and the mineral faujasite. At the right is shown the tetrahedral arrangement of truncated octahedra surrounding one large cavity. On the left the packing model of zeolite X is shown, containing three types of Na^+ cations.

MCM-68 (31) etc. The need for new materials in the zeolite has led to exploring different heteroatoms in the synthesis protocols. The incorporation of Zn in the silicate system afforded materials in novel composition range not achieved in the aluminosilicates via stabilization of primarily three rings, as well as new structural topologies eg, VPI-7, VPI-8 and VPI-9 (32).

More recently several highly siliceous zeolites have been discovered in aqueous media in the presence of fluoride ions. The fluoride ions play a significant role of a mineralizer to help crystallize zeolitic phases, another crucial parameter in this synthetic route is the higher concentration of the starting materials leading to higher nucleation rates. The zeolites prepared by this route are hydrophobic in nature and some have new structural topologies, eg, ITQ-3 and ITQ-9 (33). The introduction of heteroatoms especially Ge in these systems have resulted in new zeolites with 3D channel systems, Germanium in the presence of fluoride ions seems to help stabilize D4R in the zeolitic frameworks. The unique topology of ITQ-12 consists of small eight ring channels and ITQ-13 contains medium pores with a rather novel $10 \times 9 \times 9$ ring pore structure (34). Zeolites containing 3D large pores circumscribed by 12-membered rings are rare and at least four new materials discovered in the Ge silicate system exhibit this features ie, ITQ-7, ITQ-17, ITQ-22 and ITQ-24 (35). These materials exhibit promise as their chemical composition and structural architecture could potentially lead to new catalytic applications.

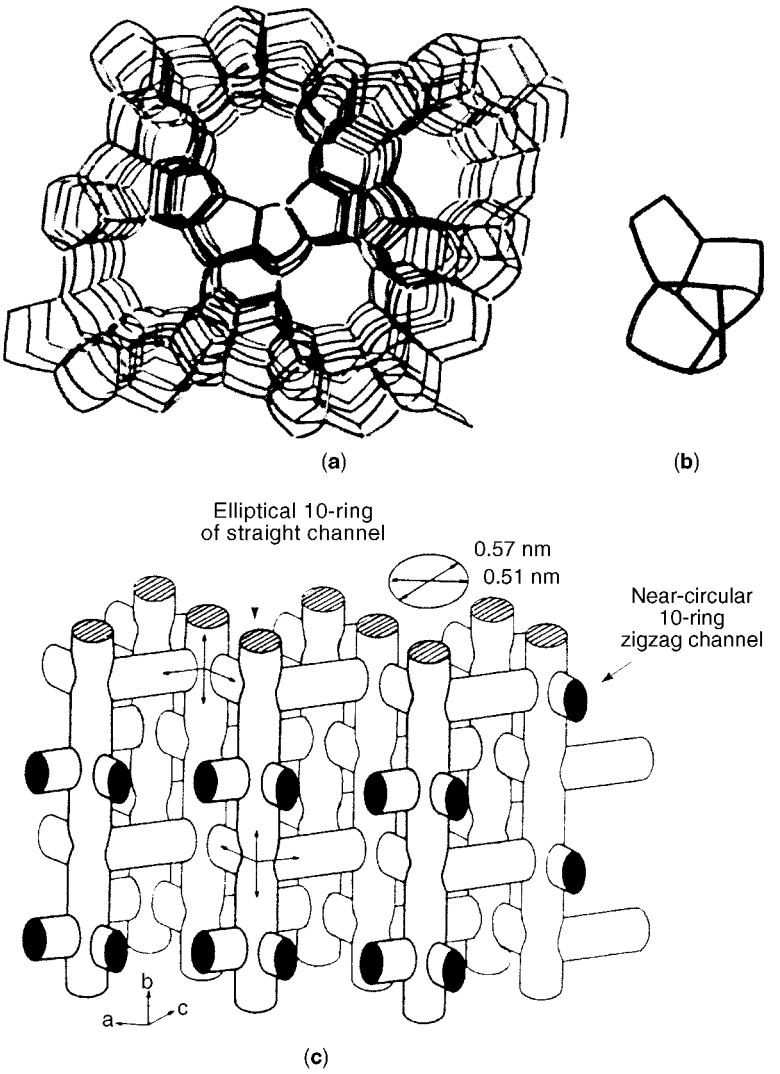

Fig. 5. (**a**) Framework structure showing the topology of the molecular sieve Z5M-5 (silicalite) viewed in the direction of the main channel. (**b**) The 12-tetrahedra secondary building unit. (**c**) Idealized channel system in ZSM-5 (28). (Courtesy of *Nature*.)

3.3. Phosphate-Containing Molecular Sieves. The discovery of novel aluminophosphate ($AlPO_4$) (2), silicoaluminophosphate (SAPO) (3), metal-containing aluminophosphate (MeAPO) (4), and metal-containing silicoaluminophosphate (MeAPSO) (5) molecular sieves announced by the Union Carbide Corp. provided an extraordinary expansion of new chemical compositions with known topologies as well as unique topologies. Table 2 lists some of these interesting materials. These materials are synthesized via techniques utilized for aluminosilicate zeolites (autoclaves, gels, etc) including the use of organic directing agents such as tri-*n*-propylamine, tetraethyl- or tetrapropylammonium, quinuclidine, etc.

Table 2. **List of Phosphate-Containing Molecular Sieves**[a]

Framework designation	Topology	Ring size	Pore diameter, nm
AlPO-5	novel	12	0.73×0.73
AlPO-8	novel	14	0.79×0.87
AlPO-11	novel	10 puckered	0.40×0.67
AlPO-17	Erionite	8	0.43
AlPO-20	Sodalite	6	0.26
AlPO-31	novel	12	0.54×0.54
AlPO-41	novel	10	4.3×7.0
SAPO-5	novel	12	0.73×0.73
SAPO-11	novel	10 puckered	0.4×0.67
SAPO-20	Sodalite	6	0.3
SAPO-34	Chabazite	8	0.43
SAPO-35	Levynite	8	0.43
SAPO-37	Faujasite	12	0.74
SAPO-40	novel	12	0.67×0.69
SAPO-42	Zeolite A	8	0.43
CoAPO-50	novel	12, 8	0.61, 0.40×0.43

[a]Thirteen structures of various compositions, as AlPO, SAPO, MeAPO, and MeAPSO, are available from UOP.

The introduction of phosphate into the framework has led to an extraordinary expansion of the possible pore diameters in framework molecular sieves. The discovery of VPI-5, the first 18-membered ring aluminophosphate framework, was a landmark (11). Although it is a neutral framework, it pointed to the possibility of larger pore-diameter materials. Since the VPI-5 discovery, at least two new phosphate structures have been announced: Cloverite, a 20-membered ring gallophosphate (12), and JDF-20 (36), a 20-membered ring aluminophosphate. Beryllo- and zinco-phosphate versions of faujasite have been reported (37). The expansion of the synthesis window to include metal containing aluminophosphate has generated a number of multi-dimensional large pore materials: UCSB-6 and UCSB-8 (38), however, these materials do not exhibit thermal stability thus have limited potential.

Over the past few years some of the SAPOs have demonstrated as excellent catalyst for hydrocarbon conversions especially where mild acidity and unique structural attributes are essential. The catalyst for methanol to olefins (MTO) process developed by UOP is based on a SAPO-34 chabazite structure with unique cage and small pore opening as well as the dewaxing catalyst licensed by Chevron a uni-dimensional SAPO-11 with elliptical 10 MR pores.

3.4. Structure Modification. Several types of structural defects or variants can occur, which figure in adsorption and catalysis: (*1*) surface defects due to termination of the crystal surface and hydrolysis of surface cations; (*2*) structural defects due to imperfect stacking of the secondary units, which may result in blocked channels; (*3*) ionic species, eg, OH^-, AlO_2^-, Na^+, SiO_4^{4-}, may be left stranded in the structure during synthesis; (*4*) the cation form, acting as the salt of a weak acid, hydrolyzes in aqueous suspension to produce free hydroxide and cations in solution; and (*5*) hydroxyl groups in place of metal cations may be introduced by ammonium ion exchange, followed by thermal deammoniation.

4. Properties

4.1. Adsorption. Although several types of microporous solids are used as adsorbents for the separation of vapor or liquid mixtures, the distribution of pore diameters does not enable separations based on the molecular-sieve effect. The most important molecular-sieve effects are shown by crystalline zeolites, which selectively adsorb or reject molecules based on differences in molecular size, shape, and other properties such as polarity. The sieve effect may be total or partial.

Activated diffusion of the adsorbate is of interest in many cases. As the size of the diffusing molecule approaches that of the zeolite channels, the interaction energy becomes increasingly important. If the aperture is small relative to the molecular size, then the repulsive interaction is dominant and the diffusing species needs specific activation energy to pass through the aperture. Similar shape-selective effects are shown in both catalysis and ion exchange, two important applications of these materials (39).

During the adsorption or occlusion of various molecules, the micropores fill and empty reversibly. Adsorption in zeolites is a matter of pore filling, and the usual surface area concepts are not applicable. The pore volume of a dehydrated zeolite and other microporous solids which have type I isotherms may be related by the Gurvitch rule, ie, the quantity of material adsorbed is assumed to fill the micropores as a liquid having its normal density. The total pore volume V_p is given by

$$V_p = x_s/d_a$$

where d_a = the density of the liquid adsorbate in g/cm^3, x_s = amount adsorbed at saturation in g/g, and V_p in cm^3/g.

The channels in zeolites are only a few molecular diameters in size, and overlapping potential fields from opposite walls result in a flat adsorption isotherm, which is characterized by a long horizontal section as the relative pressure approaches unity (Fig. 6). The adsorption isotherms do not exhibit hysteresis as do those in many other microporous adsorbents. Adsorption and desorption are reversible, and the contour of the desorption isotherm follows that of adsorption.

In order to utilize the absorption properties of the synthetic zeolite crystals in processes, the commercial materials are prepared as pelleted aggregates combining a high percentage of the crystalline zeolite with an inert binder. The formation of these aggregates introduces macropores in the pellet that may result in some capillary condensation at high adsorbate concentrations. In commercial materials, the macropores contribute diffusion paths. However, the main part of the adsorption capacity is contained in the voids within the crystals.

Zeolites are high capacity, selective adsorbents capable of separating molecules based on the size and shape of the molecule relative to the size and geometry of the main apertures of the structure. They adsorb molecules, in particular those with a permanent dipole moment which show other interaction effects, with a selectivity that is not found in other solid adsorbents. Separation may be based on the molecular-sieve effect or may involve the

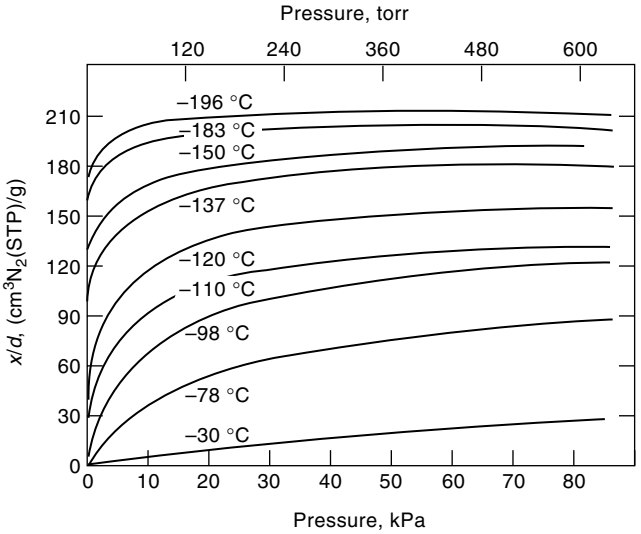

Fig. 6. Family of adsorption isotherms for adsorption of nitrogen on zeolite X at temperatures of −30 to 196°C (1).

preferential or selective adsorption of one molecular species over another. These separations are governed by several factors. The basic framework structure, or topology, of the zeolite determines the pore size and the void volume. The exchange cations, in terms of their specific location in the structure, their population density, their charge and size, affect the molecular-sieve behavior and adsorption selectivity of the zeolite. By changing the cation types and number, the selectivity of the zeolite in a given separation can be tailored or modified, within certain limits.

The cations, depending on their locations, contribute electric field effects that interact with the adsorbate molecules. The effect of the temperature of the adsorbent is pronounced in cases involving activated diffusion. Sieving by dehydrated zeolite crystals is based on the size and shape differences between the crystal apertures and the adsorbate molecule. The aperture size and shape in a zeolite may change during dehydration and adsorption because of framework distortion or cation movement. In some instances, the aperture is circular, such as in zeolite A. In others, it may take the form of an ellipse such as in dehydrated chabazite. In this case, subtle differences in the adsorption of various molecules result from a shape factor. Some typical molecular dimensions are shown in Figure 7, based on the Lennard-Jones (39–44) potential function (1).

As shown in Figure 7, the calcium-exchanged form of zeolite A has a pore diameter of 0.42 nm, which compares well with the value of 0.43 nm for the kinetic diameter of normal paraffin hydrocarbons and 0.44 nm for dichloromethane, both of which are absorbed. The apparent pore size, therefore, varies between 0.42 and 0.44 nm. This molecular sieve is referred to as 5A. For the sodium A zeolite (NaA), because of the higher cation population, the apparent pore diameter is 0.36–0.40 nm, depending on temperature (4A). The potassium form of zeolite A (KA), when highly exchanged, adsorbs some carbon dioxide

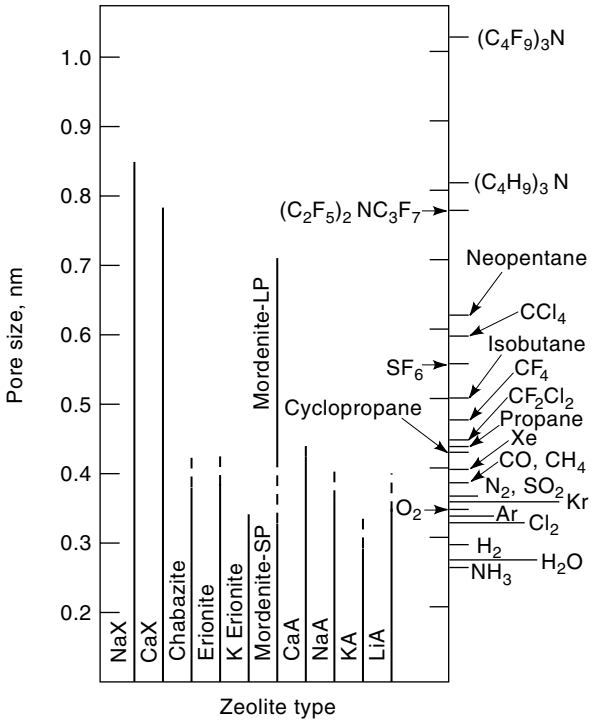

Fig. 7. Molecular dimension and zeolite pore size. Chart showing a correlation between effective pore size of various zeolites over temperatures of 77–420 K (- - -) with the kinetic diameters of various molecules (1). M–A is a cation–zeolite A system. M–X is a cation–zeolite X system.

and, at lower degrees of exchange, ethylene. A pore diameter of 0.33 nm is appropriate to these results (3A).

The zeolite sodium X (type 13X) has a crystallographic aperture of 0.74 nm. This compares well with the adsorbate value of 0.81 nm. Zeolite calcium X exhibits a smaller apparent pore size of 0.78 nm (10X). This difference is probably due to some distortion of the aluminosilicate framework upon dehydration and calcium ion migration.

When two or more molecular species involved in a separation are both adsorbed, selectivity effects become important because of interaction between the zeolite and the adsorbate molecule. These interaction energies include dispersion and short-range repulsion energies (φ_D and φ_R), polarization energy (φ_P), and components attributed to electrostatic interactions.

4.2. Types of Separations. The first type of adsorption separation is based on differences in the size and shape of molecules (1,41). The molecular sieve separation of hydrocarbons by zeolite calcium A (5A) is used in commercial processes for the recovery of normal paraffins from hydrocarbon feedstocks (45) (see ADSORPTION, LIQUID SEPARATION). Paraffin isomers and cyclic hydrocarbons are too large to be adsorbed and are excluded. The recovered *n*-paraffins are utilized, eg, in the manufacture of biodegradable detergents. The affinity of zeolites for water and other polar molecules decreases with rising SiO_2/Al_2O_3. Therefore,

low silica zeolites can be used for drying gases and liquids. However, in many instances, secondary reactions such as polymerization of a coadsorbed olefin may take place. This is avoided by using the potassium-exchanged form of zeolite A (3A) for the removal of water from unsaturated hydrocarbon streams. The effective pore size of 3A excludes all hydrocarbons, including ethylene. The molecular-sieve effect for water removal is also utilized in the drying of refrigerants. In this instance, zeolite A (4A) is employed because the size of the refrigerant molecules, such as refrigerant-12 with a kinetic diameter of 0.44 nm, is too large to be adsorbed. The second type of adsorption separation is based on differences in the relative selectivity of two or more coadsorbed gases or vapors. An outstanding example of this type is the production of oxygen-enriched air by the selective adsorption of nitrogen at ambient temperature on various molecular-sieve zeolites, including calcium A, calcium X, and various types of mordenite. Many separations based on relative selectivity range from simple drying processes to the separation of sulfur compounds from natural gas, and of aromatics from saturated hydrocarbons.

4.3. Tailoring of Zeolite Adsorption Selectivities. It is possible to tailor the zeolite adsorption characteristics in terms of size selectivity or the selectivity caused by other interactions, including cation exchange; cation removal or decationization; the presorption of a very strongly held polar molecule, such as water; pore-closure effects, that is, effects that alter the size of the openings to the internal pore volume; and the introduction of various defects such as removal of framework aluminum and an increase in the silicon/aluminum ratio (42). When synthetic mordenite is dealuminated by acid treatment, the SiO_2/Al_2O_3 ratio can increase to ~ 100 with the result that the water-adsorption capacity is essentially eliminated, and the zeolite becomes hydrophobic (42). The limit is attained in high silica ZSM-5 also known as silicalite. This material is capable of removing organic compounds from water (28).

4.4. Adsorption Kinetics. In zeolite, adsorption processes the adsorbates migrate into the zeolite crystals. First, transport must occur between crystals contained in a compact or pellet, and second, diffusion must occur within the crystals. Diffusion coefficients are measured by various methods, including the measurement of adsorption rates and the determination of jump times as derived from nmr results. Factors affecting kinetics and diffusion include channel geometry and dimensions; molecular size, shape, and polarity; zeolite cation distribution and charge; temperature; adsorbate concentration; impurity molecules; and crystal-surface defects.

4.5. Catalytic Properties. In zeolites, catalysis takes place preferentially within the intracrystalline voids. Catalytic reactions are affected by aperture size and type of channel system, through which reactants and products must diffuse. Modification techniques include ion exchange, variation of Si/Al ratio, hydrothermal dealumination or stabilization, which produces Lewis acidity, introduction of acidic groups such as bridging Si(OH)Al, which impart Brönsted acidity, and introducing dispersed metal phases such as noble metals. In addition, the zeolite framework structure determines shape-selective effects. Several types have been demonstrated including reactant selectivity, product selectivity, and restricted transition state selectivity (46). Nonshape-selective surface activity is observed on very small crystals, and it may be desirable to poi-

son these sites selectively, eg, with bulky heterocyclic compounds unable to penetrate the channel apertures, or by surface silation.

Some current and possible future zeolite catalyst applications are as follows: alkylation, cracking, hydrocracking, dewaxing, isomerization, hydrogenation and dehydrogenation, hydrodealkylation, methanation, shape-selective reforming, dehydration, methanol to gasoline, methanol to olefins, organic catalysis, inorganic reactions, H_2S oxidation, NH_3 reduction of NO, $H_2O \rightarrow 1/2O_2 + H_2$ and CO oxidation.

4.6. Acid Sites. Acidic zeolites have outstanding catalytic activity. The hydrogen form may be produced by ammonium ion exchange, followed by thermal deammoniation. The unsolvated proton forms an OH group with a bridging O:

$$\equiv SiH-O-Al\equiv \xrightleftharpoons[+NH_3]{NH_4^+ \quad -NH_3} [\equiv SiH-O-Al\equiv] \xrightleftharpoons{H^+} \equiv SiH-OH-Al\equiv$$

The presence of an electron donor causes the equilibrium to shift to the left. The acidity represented by this mechanism is important in hydrocarbon conversion reactions. Acidity may also be introduced in certain high silica zeolites, eg, mordenite, by hydrogen-ion exchange, or by hydrolysis of a zeolite containing multivalent cations during dehydration, eg,

$$Ce^{3+}Z + H_2O \longrightarrow Ce(OH)^{2+}HZ$$

where Z = zeolite. The number and acid strength of these Brönsted acid sites are both important. The hydroxyl groups thus generated have been well characterized by several techniques, eg, ir spectroscopy. It has been demonstrated, eg, that the acid hydroxyl groups have a characteristic frequency that is determined by the charge density of the framework (43). Lewis sites may be generated by the formation of hexacoordinated aluminum atoms at cationic positions in extralattice positions (43).

4.7. Stabilized Zeolites. It is desirable that a zeolite to be used as a catalyst be stable during reaction and regeneration. For many catalytic applications, adequate thermal and hydrothermal stability of the zeolite is required. The structural stability of a zeolite, eg, zeolite Y, increases with Si/Al ratio. Further stabilization, particularly of the acid function, can be achieved by exchange with polyvalent cations such as rare-earth ions. Mixed rare-earth-exchanged zeolite Y is used in cracking catalysts. Increased stability is also obtained by hydrothermal treatment of the ammonium or rare-earth-exchanged form. When heated at high temperatures in the presence of water vapor, tetrahedral aluminum atoms are removed from the framework by hydrolysis with the formation of extra-framework cationic Al species such as $Al(OH)^{2+}$ or AlO^+, which impart additional structural and acid stability (47). The stabilizing effect of aluminum cations is similar to that of rare-earth cations. Such cationic aluminum species can be removed by ion exchange. Careful chemical treatment with acids or chelating agents may also be used to dealuminate the framework (48).

In shape-selective catalysis, the pore size of the zeolite is important. For example, the ZSM-5 framework contains 10-membered rings with ~0.6 nm pore size. This material is used in xylene isomerization, ethylbenzene synthesis, dewaxing of lubrication oils and light fuel oil, ie, diesel and jet fuel, and the conversion of methanol to liquid hydrocarbon fuels (39).

The zeolites used for catalysis are principally modified forms of zeolite Y, acid forms of synthetic mordenite, ferrierite, ZSM-5 and MCM-22.

4.8. Dispersed Metals. Bifunctional zeolite catalysts, principally zeolite Y, are used in commercial processes such as hydrocracking. These are acidic zeolites containing dispersed metals such as platinum or palladium. The metals are introduced by cation exchange of the amine complexes, followed by a reductive decomposition (39):

$$Na_2Y + Pt(NH_3)_4^{2+} \longrightarrow Pt(NH_3)_4^{2+}Y^{2-} + 2\,Na^+$$

$$Pt\Big(NH_3\Big)_4^{2+}Y^{2-} + H_2 \longrightarrow Pt^0(H^+)_2Y^{2-} + 4\,NH_3$$

A bidisperse system involving metal agglomerates in the supercages and some crystallites at the external surface is commonly the result of this reaction. This migration during reduction with hydrogen may be attributable to formation of mobile platinum hydride, $Pt(NH_3)_2H_2$. Migration can be prevented by adding an olefin, which appears to act as a hydride trap, to the hydrogen gas (49). Other transition metal ions such as Cd, Zn, Ni, and Ag are introduced by ion exchange followed by reduction with hydrogen. Agglomeration and migration to the external surface can also occur with these metals. Dehydrated zeolites can be loaded with metals by adsorption of neutral compounds such as carbonyls, followed by thermal decomposition. Molybdenum, ruthenium, and nickel have been loaded by this method into large-pore zeolites (44).

4.9. Ion Exchange. The exchange behavior of nonframework cations in zeolites, eg, selectivity and degree of exchange, depends on the nature of the cation, eg, the size and charge of the hydrated cation, on the temperature, the concentration, and, to some degree, on the anion species. Cation exchange may produce considerable change in various other properties, such as thermal stability, adsorption behavior, and catalytic activity.

The ion-exchange process is represented by

$$Z_A B^{Z_B}(z) + Z_A Z_B A^{Z_A}(s) \rightleftarrows Z_A B^{Z_B}(s) + Z_B A^{Z_A}(z)$$

where Z_A and Z_B are the ionic charge of cations A and B and (z) and (s) represent the zeolite and solution. The ion-exchange isotherm (Fig. 8) is constructed by plotting A_z versus A_s, where A_z and A_s represent the mole fractions of cation A in the zeolite and solution, respectively. Similarly, with B_z and B_s represent the mole fractions of cation A in the zeolite and solution, respectively. Similarly, with B_z and B_s representing the mole fraction of cation B in the zeolite and solution, the preference of the zeolite for ion A is given by the separation factor:

$$\alpha_B^A \equiv \frac{A_z B_s}{B_z A_s}$$

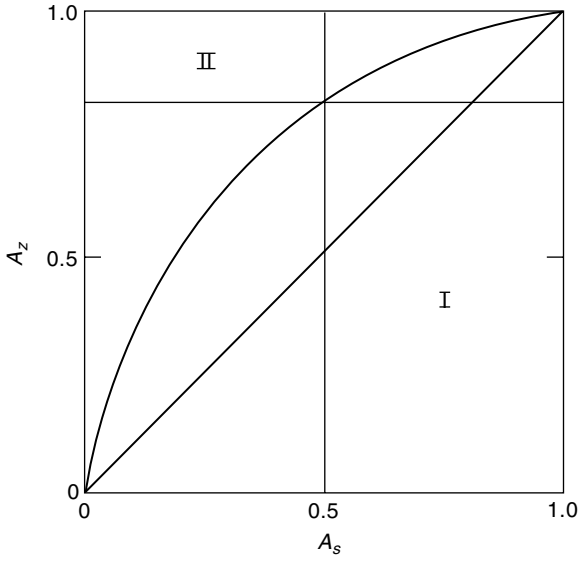

Fig. 8. Ion-exchange isotherm. The separation factor $\alpha^{A}{}_{B}$ is given by the ratio of area I/area II (1). See text.

Ion-exchange isotherms assume different shapes depending on the selectivity factor and the variations in A_s with the level of exchange A_z. The rational selectivity coefficient $K^{A}{}_{B}$ includes the ionic charge and is given by

$$K_B^A \equiv \frac{A_z^{Z_B} B_s^{Z_A}}{B_z^{Z_A} A_s^{Z_B}}$$

Typical exchange isotherms are given in Figure 9 for zeolite X. The exchange capacity of various zeolites is given in Table 3. In many cases, complete exchange does not take place, such as for dipositive and tripositive ions in zeolite Y because of nonoccupancy of cation sites type I and I′, located in the small cages. This corresponds to a maximum level of 0.68. Similarly, the level of exchange diminishes with the size and volume of the cation since the intracrystalline volume available does not permit full cation-site occupancy.

4.10. Kinetics. Ion-exchange rates in zeolites are controlled by ion diffusion within the zeolite structure, and are affected by particle radii, ionic diffusion coefficients, and temperature. For example, in zeolite NaX, diffusion of sodium ions occurs by migration from type II sites (in the six-membered rings) into the large cages, followed by diffusion to the surface through the large channels. As a result, complete replacement of sodium by calcium can be accomplished only at elevated temperatures.

4.11. Selectivity. Cation sieving in zeolites is attributed to cation size, distribution of charge in the zeolite structures, and size of the hydrated ion in aqueous solution. Solvation influences exchange since, for the ion to diffuse into the crystal, exchange of solvent molecules such as H_2O must always occur.

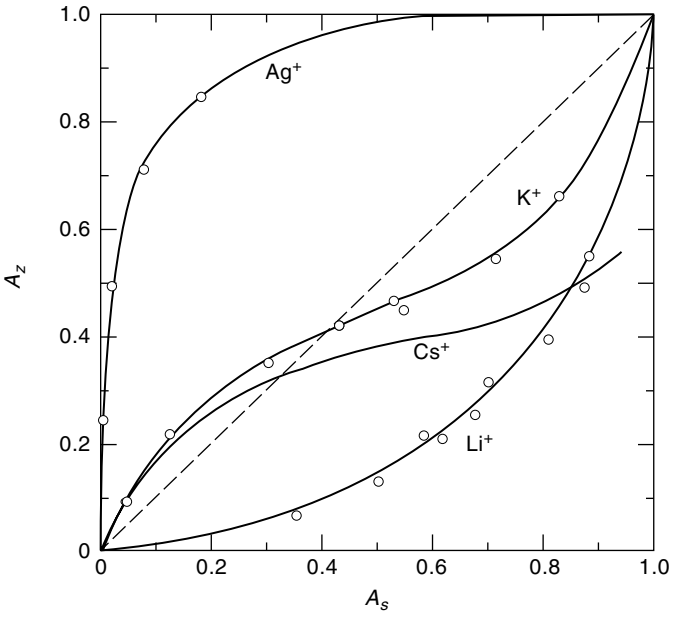

Fig. 9. Ion-exchange isotherms on zeolite X, sodium form.

Table 3. **Ion-Exchange Capacity of Various Zeolites**[a]

Zeolite	Si/Al ratio	meq/g
chabazite	2	5
mordenite	5	2.6
erionite	3	3.8
clinoptilolite	4.5	2.6
zeolite A	1	7.0
zeolite X	1.25	6.4
zeolite Y	2.0	5.0
ZSM-5	2.0	0.78
ZSM-5	3.5	0.46

[a]Anhydrous powder basis.

The selectivity coefficient K^{A}_{B} varies with the Si/Al ratio of the zeolite. In zeolites A (Si/Al = 1) and X (Si/Al = 1.2), the selectivity series for unipositive ions is Na > K > Rb > Cs. In zeolite Y (Si/Al = 2.8), the selectivity series is Cs > Rb > K > Na > Li. Even in unipositive–dipositive ion exchange, the normal preference for the dipositive ion shown by zeolites A and X is reversed in zeolites with Si/Al ratio of ~3.

5. Framework Modification

The zeolite framework can be stabilized by hydrothermal treatment, which removes aluminum from the framework and forms aluminum cations. During

this steaming process, the tetrahedral vacancies left behind in the framework are gradually refilled with silicon, which appears to migrate as a form of silicic acid from other parts of the framework and contributes to the stabilization by repairing the damaged framework. Simultaneously, such other parts of the framework disappear under formation of mesopores (50). Cationic aluminum can be extracted with an acid, and a subsequent steaming causes further dealumination of the framework and migration of silicon into the vacancies. Carefully controlled conditions can produce high silica forms of zeolites, eg, zeolite Y (51). Since the Si−O bond is shorter than the Al−O bond, hydrothermal dealumination causes the unit cell parameter to decrease.

Mesopores can be avoided by replacing the aluminum directly with external silicon, eg, by treatment with silicon tetrachloride (52):

$$\mathrm{Na}\left[\mathrm{AlO_2(SiO_2)}_x\right] + \mathrm{SiCl_4} \longrightarrow \left[(\mathrm{SiO_2})_{x+1}\right] + \mathrm{NaAlCl_4}$$

$NaAlCl_4$ formed in this process needs to be removed by washing with water, in order to achieve the desired improved stability. A more convenient method for replacing framework-Al with Si is the reaction with ammonium hexafluorosilicate (53).

In a reversal of the reaction with $SiCl_4$, aluminum can be introduced into the framework by reaction of the hydrogen or ammonium form with gaseous $AlCl_3$ (54). Similarly, reaction with aqueous ammonium fluoroaluminates replaces framework-Si with Al (55). When alumina-bound high silica zeolites are hydrothermally treated, aluminum migrates into framework positions and generates catalytically active acid sites (56). The reaction can be accelerated by raising the pH of the aqueous phase.

The presence of internal silanol groups (57) and hydroxyl nests (58) in high silica zeolites facilitates the insertion of aluminum (hydroxyl nests can be generated, eg, by facile removal of boron from the framework of [B]ZSM-5). In analogy to the reaction with $AlCl_3$, boron, gallium, and indium have been inserted into the zeolite framework by treatment with the respective chlorides (59). Beryllium has been inserted by treatment with $(NH_4)_2BeF_4$ (60). Although some insertion of Fe may have been achieved, Fe, Cr, and Ti are incompletely inserted, or grafted to silanol groups by treatment with the respective complex fluorides.

6. Manufacture

Zeolites are formed under hydrothermal conditions, defined here in a broad sense to include zeolite crystallization from aqueous systems containing various types of reactants. Most synthetic zeolites are produced under nonequilibrium conditions, and must be considered as metastable phases in a thermodynamic sense.

More than 150 synthetic zeolites have been reported and some important types have no natural mineral counterpart or are found in scarce amounts in remote locations not economical to mine. Conversely, synthetic counterparts of many zeolite minerals are not yet known. The conditions generally used in synthesis are reactive starting materials such as freshly coprecipitated gels, or amorphous solids; relatively high pH introduced in the form of an alkali metal

hydroxide or other strong base, including tetraalkylammonium hydroxides; low temperature hydrothermal conditions with concurrent low autogenous pressure at saturated water vapor pressure; and a high degree of supersaturation of the gel components, leading to nucleation of a large number of crystals.

A gel is defined as a hydrous metal aluminosilicate prepared from either aqueous solutions, reactive solids, colloidal sols, or reactive aluminosilicates such as the residue structure of metakaolin and glasses.

The gels are crystallized in a closed hydrothermal system at temperature varying from room temperature to ~200°C. The time required for crystallization varies from a few hours to several days. When prepared, the aluminosilicate gels differ in appearance, from stiff and translucent to opaque gelatinous precipitates and heterogeneous mixtures of an amorphous solid dispersed in an aqueous solution. The alkali metals form soluble hydroxides, aluminates, and silicates. These materials are well suited for the preparation of homogeneous mixtures.

Gel preparation and crystallization is represented schematically using the $Na_2O–Al_2O_3–SiO_2–H_2O$ system as an example (1).

$$\mathrm{NaOH\ (aq) + NaAl(OH)_4(aq) + Na_2SiO_3(aq) \xrightarrow{25^\circ C} \left[Na_a(AlO_2)_b(SiO_2)_c \cdot NaOH \cdot H_2O\right]}$$

$$\mathrm{gel \xrightarrow{25–175^\circ C} Na_x \left[(AlO_2)_x(SiO_2)_y\right] \cdot mH_2O}$$

Typical gels are prepared from aqueous solutions of reactants such as sodium aluminate, NaOH, and sodium silicate; other reactants include alumina trihydrate ($Al_2O_3 \cdot 3H_2O$), colloidal silica, and silicic acid. Some synthetic zeolites prepared from sodium aluminosilicate gels are given in Table 4.

When the reaction mixtures are prepared from colloidal silica sol or amorphous silica, additional zeolites may form that do not readily crystallize from the homogeneous sodium silicate–aluminosilicate gels. The temperature strongly influences the crystallization time of even the most reactive gels; eg, zeolite X crystallizes in 800 h at 25°C and in 6 h at 100°C.

Synthesis mechanisms of the typical low silica zeolites, such as A, X, and Y, are apparently different from the high silica zeolites such as ZSM-5. In the low silica zeolites, nuclei are formed consisting of alkali metal-ion complexes of the aluminosilicate species. Structural units consisting of four-membered rings, six-membered rings, and cages coordinated with cations are thought to be involved in the nucleation and crystallization. In the high silica zeolites, the mechanism appears to be a templating type (61), where an alkylammonium cation complexes with silica by hydrogen bonding. These complexes cause the structures to replicate by hydrogen bonding of the organic cation with framework oxygen atoms (62).

In general, zeolite crystallization consists of three stages: (*1*) formation of precursors, ie, building blocks that can generate nuclei; (*2*) nucleation; and (*3*) crystal growth.

X-ray diffraction can monitor only the progress of crystal growth, and stages 1 and 2 are frequently combined as the "induction period" (63). Nucleation without appreciable crystal growth can be accomplished by aging at low temperatures, eg, room temperature for zeolite Y, while crystal growth is accelerated at

Table 4. **Some Synthetic Zeolites Prepared from Sodium Aluminosilicate Gels**

Zeolite type	Typical composition, mol/mol Al_2O_3			Reactants	Temp, °C	Zeolite product composition, mol/mol Al_2O_3		
	Na_2O	SiO_2	H_2O			Na_2O	SiO_2	H_2O
A	2	2	35	$NaAlO_2$, NaOH, Sodium silicate	20–175	1	2	4.5
X	3.6	3	144	$NaAlO_2$, NaOH, Sodium silicate	20–120	1	2–3	6
Y	8	20	320	$NaAlO_2$, colloidal SiO_2	20–175	1	3–6	9
mordenite zeolon	6.3	27	61	$NaAlO_2$, diatomite, Sodium silicate	100	1	9–10	6.7
omega	5.6[a]	20	280	colloidal SiO_2, NaOH, $Al(OH)_3$, TMAOH[b]	100	0.71 0.36 (TMA)	0.73	6.3
ZSM-5	10[c]	7.7	453	$NaAlO_2$, SiO_2, TPAOH[e]	150	0.89	31.1[d]	

[a] Also 1.4 TMA_2O.
[b] TMA = tetramethylammonium.
[c] Also 8.6 TPA_2O.
[d] After calcination at 1000°C.
[e] TPA = tetrapropylammonium.

high temperatures. In some cases, crystallization of a zeolitic impurity can be prevented by aging. Another method for inducing crystal growth is seeding, ie, the introduction of seed crystals or precrystal nuclei. Using this procedure, the induction period is eliminated, and crystal growth starts immediately, so that the crystallization of the desired zeolite may be complete before nucleation of a zeolitic impurity reaches a stage at which growth commences (Fig. 10) (64).

6.1. Processes. Manufacturing processes for commercial molecular sieve products may be classified into three groups, as shown in Table 5 (1): the preparation of molecular sieve zeolites as high purity crystalline powders or as preformed pellets from reactive aluminosilicate gels or hydrogels; the conversion of clay minerals into zeolites, either in the form of high purity powders or as binderless high purity preformed pellets; and processes based on the use of other naturally occurring raw materials. The hydrogel and clay conversion processes may also be used to manufacture products that contain the zeolite as a major or a minor component in a gel matrix, a clay matrix, or a clay-derived matrix. Powdered products are often bonded with inorganic oxides or minerals into agglomerated particles for ease in handling and use.

6.2. Hydrogel Processes. The first commercial process for preparing synthetic zeolites on a large scale was based on a laboratory synthesis using

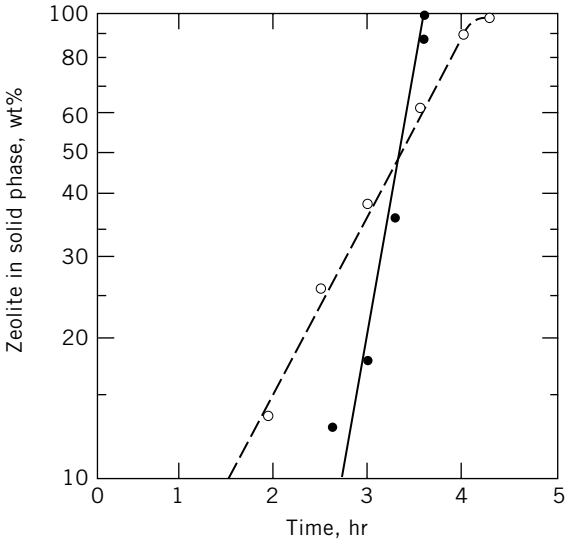

Fig. 10. The growth of (○) zeolite X and (●) zeolite B (64). Prenucleation or seeding of zeolite X moves the growth curve to the left.

amorphous hydrogels. The typical starting materials included an aqueous solution of sodium silicate, sodium aluminate, and sodium hydroxide. Hydrogel processes are based either on homogeneous gels, ie, hydrogels prepared from solutions of soluble reactants, or on heterogeneous hydrogels which are prepared from reactive alumina or silica in a solid form, eg, solid amorphous silica powder.

In gel-forming processes, the reactive aluminosilicate gel is first formed into a pellet that reacts with sodium aluminate solution and caustic solution. The zeolite crystallizes *in situ* within an essentially self-bonded pellet, or as a component in an unconverted amorphous matrix.

Table 5. **Processes for Molecular Sieve Zeolites**

Process	Reactants	Products
hydrogel	reactive oxides	high purity powders
	soluble silicates	gel preform
	soluble aluminates	zeolite in gel matrix
	caustic	
clay conversion	raw kaolin	low to high purity powder
	meta-kaolin	binderless, high purity preform
	acid-treated clay	zeolite in clay derived matrix
	soluble silicate	
	caustic	
	sodium chloride	
other	natural SiO_2	low to high purity powder
	amorphous minerals	zeolite on ceramic support
	volcanic glass	binderless preforms
	caustic	

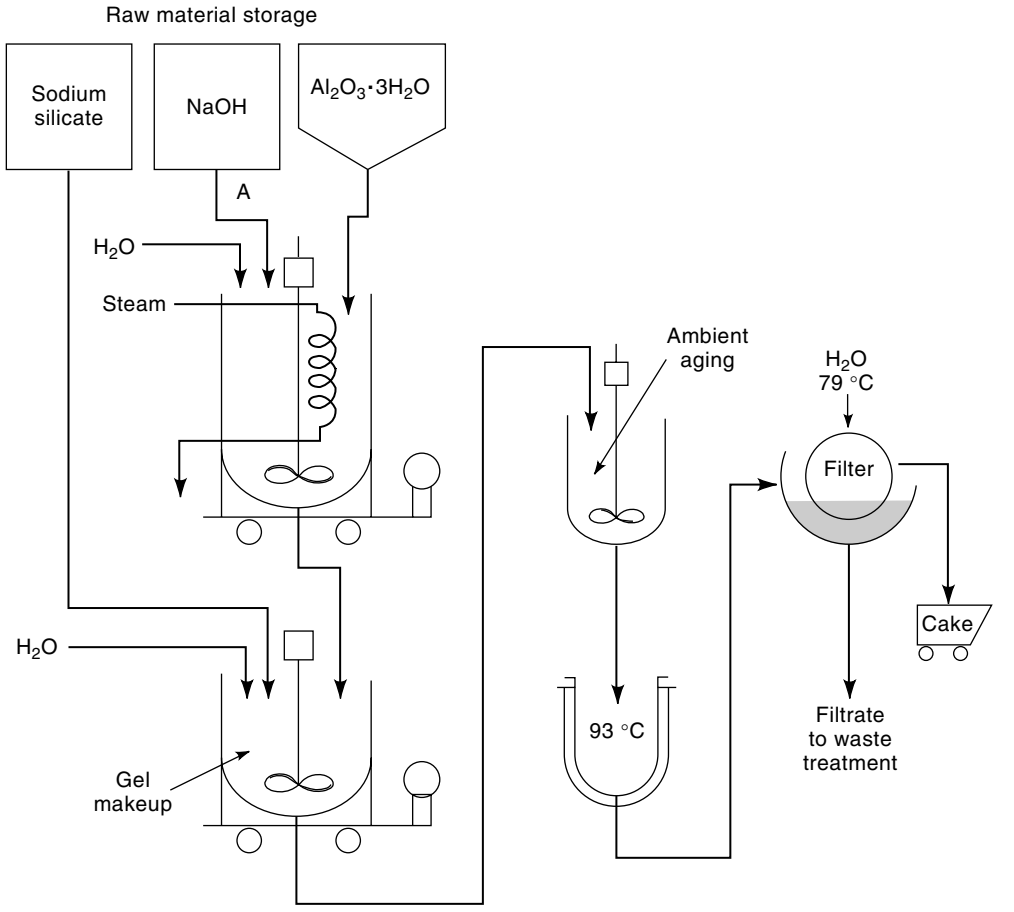

Fig. 11. Hydrogel process. Process flow sheet for the manufacture of zeolites 4A, 13X, and Y from reactant hydrogels (1).

A process flow sheet for the manufacture of types 4A, 13X, and Y as high purity crystalline zeolite powders is shown in Figure 11.

Typical material balances as well as chemical compositions are given in Table 6. The raw materials are metered into the makeup tanks in the proper ratios. Crystallization takes place in a separate crystallizer. An intermediate aging step at ambient temperature may be required for the synthesis of certain high purity zeolites.

The process appears to be simple in terms of equipment and experimental conditions; however, because of the metastability of zeolite species formed from typical reactant systems, problems may arise when large-scale synthesis is attempted. For low silica zeolites, the crystallization temperature is usually near the boiling point of water; higher temperatures are commonly applied in the synthesis of high silica zeolites. After the digestion period, the slurry of crystals in the mother liquor is filtered in a rotary filter.

Table 6. **Typical Material Balance for Hydrogel Process, kg**[a]

	Zeolite		
Raw materials	A	X	Y
sodium silicate[b]	1350	2000	
SiO_2 powder[c]			1450
alumina trihydrate[d]	575	500	340
caustic, 50% NaOH	870	1600	1400
water	3135	7687	5300
Na_2O	2.04	4.09	4.0
Al_2O_3	1	1	1
SiO_2	1.75	3.0	10.6
H_2O	70	176	161

[a]To produce 1000 kg, dry basis.
[b]9.4% Na_2O, 28.4% SiO_2.
[c]95% SiO_2.
[d]65% Al_2O_3, 35% H_2O.

6.3. Clay Conversion. The starting material for this process is kaolin, which usually must be dehydroxylated to *meta*-kaolin by air calcination. At 500–600°C, *meta*-kaolin forms, followed by a mullitized kaolin at 1000–1050°C.

$$\underset{\text{kaolin}}{Al_2Si_2O_5(OH)_4} \xrightarrow{1050^\circ C} \underset{\text{meta-kaolin}}{Al_2Si_2O_7} + 2\,H_2O$$

$$\underset{\text{meta-kaolin}}{3\,Al_2Si_2O_7} \xrightarrow{1050^\circ C} \underset{\text{mullite}}{Si_2Al_6O_{13}} + \underset{\text{cristobalite}}{4\,SiO_2}$$

The zeolites are prepared as essentially binderless preformed particles. The kaolin is shaped in the desired form of the finished product and is converted *in situ* in the pellet by treatment with suitable alkali hydroxide solutions. Preformed pellets of zeolite A are prepared by this method. These pellets may be converted by ion exchange to other forms such as molecular sieve Type 5A (1). Zeolites of higher SiO_2/Al_2O_3 ratios, eg, zeolite Y, can be obtained by the same method, when sodium metasilicate is incorporated in the preshaped pellets, or when acid-leached metakaolin is used.

6.4. Agglomeration of Synthetic Zeolite Powders. High purity zeolite crystals used in adsorption processing must be formed into agglomerates having high physical strength and attrition resistance. The crystalline powders are blended with an inorganic binder, generally a clay for adsorbents or, eg, alumina for catalysts, and wetted. The kneaded binder–zeolite–water mixture is extruded into cylindrical pellets that are subsequently calcined to form a strong composite. Or an aqueous binder–zeolite slurry is spray dried to form a fluid catalyst in the shape of microspheres.

The preparation of zeolite–binder agglomerates as spheres or cylindrical pellets having high mechanical attrition resistance is not difficult. However, in order to utilize the zeolite in a process of adsorption or catalysis, the diffusion characteristics must not be unduly affected. Consequently, the binder system

must permit a macroporosity that does not unduly increase diffusion resistance. The problem, therefore, is to optimize the binder–zeolite combination to achieve a particle of maximum density (to produce a high volumetric adsorption capacity) with maximum mechanical attrition resistance and minimum diffusion resistance.

7. Economic Aspects

Zeolites have high potential for protecting ecosystems, from facilitating wastewater and gas treatment to providing water softeners in detergents to replace the undesirable polyphosphate.

Catalytic cracking is an example of a use in which zeolites have had great impact on both crude oil and cracking unit economy. The application of zeolites made it possible to greatly increase catalytic activity, which allowed further improvement in fluid catalytic cracking (FCC) riser technology. Simultaneously, the cracking reactions became much more selective for desired products such as gasoline, while coke and gas productions were reduced. The gasoline yield improvements as induced by zeolite technology since the 1960s translate into a worldwide cumulative product value of $\sim$\$1 trillion (2000). Application of zeolitic FCC catalysts permitted more economical use of crude oil resources to reach the desired gasoline output. Moreover, new zeolitic cracking catalysts were developed to produce FCC gasoline with higher octane number (65) (see CATALYSIS).

The largest volume use for synthetic zeolites is as a builder in home laundry detergent powder $\sim 1188 \times 10^3$ t in 2001. In the United States, Canada, western Europe, and Japan the use of zeolites in the detergent market is mature and average growth since 1994 has been only 0.8% annually, down from 8% during 1990–1994 and substantially lower from 20% annual growth during 1986–1990. Zeolites-builders accounted for all home laundry detergent powder use in North America and Japan and probably reached maximum market potential in western Europe with a consumption of 620×10^3 t in 2001. The second largest use of zeolites is in catalysis, mainly for cracking in the petroleum industry; this amounted to 184×10^3 t in 2001 (66). Various modified Y-type zeolite products as well as ZSM-5 used for catalytic purposes are considered specialty chemicals with relatively low production volumes, and consequently they demand much higher prices than commodity zeolites, such as zeolite A. About 92×10^3 t of synthetic zeolites was used in 2001 for adsorbents and desiccants. Both synthetic and natural zeolites are being used at $\sim$1% as supplement in animal feeds, mainly in Japan, but to some extent also in the United States. Natural zeolites have been used for various applications such as soil conditioners, pollution control and odor control agent in animal litter. The world production has remained relatively flat during the 1990s at $\sim 3{,}300 \times 10^3$ t and sell for $\sim$\$40–250/t depending on the zeolite and mesh type.

The U.S. capacity for synthetic zeolites at the end of 2001 was 276×10^3 t for detergent use 82×10^3 t for catalysts; and $\sim 42 \times 10^3$ t for use as adsorbents and desiccants. As of 2001, the price of builder-grade zeolite A to the largest customers was about \$0.547/kg on an anhydrous basis (list price: \$0.70/kg), whereas zeolite 4A adsorbent sold for \$1.90/kg as of 2001. The price of zeolite containing FCC catalyst is related to the specific type of catalyst performance and zeolite

content. The most common catalyst since 1991 was ~$1500/t on the average, ranging from $1300–1800/t for most grades.

8. Analytical Procedures

8.1. Identification. Each zeolite has a characteristic X-ray powder diffraction pattern, which is used for identification and determination of the purity or quality of zeolite present in a composite such as a catalyst. Generally, powder patterns are determined over a 2θ range of 2–56° since these materials have large unit cells and, correspondingly, exhibit the strongest lines at low diffraction angles. However, peak intensities and, to some extent, positions, vary with dehydration or cation exchange. Suitable procedures for X-ray analysis have been developed by The American Society for Testing and Materials (ASTM). Other procedures are based on vibrational spectroscopy (ir and Raman), thermal analysis, and standard chemical analyses (67). Magic angle spinning nuclear magnetic resonance spectroscopy (mas nmr) permits tetrahedrally and octahedrally coordinated aluminum to be determined separately, a procedure particularly important for evaluation of modified zeolites in catalysts (68). The location of adsorbed xenon in the zeolite cavities can be determined by Xe nmr, and the obtained data can give information about the available intracrystalline space and the presence of extraneous matter in the cavities (68).

8.2. Adsorption. The BET (Brunauer-Emmett-Teller) method for surface–area measurement commonly employed to characterize adsorbents and catalysts is not relevant for zeolites, since adsorption on zeolites occurs by a pore-filling mechanism. Oxygen adsorption at low temperature (−183°C) is employed as a method for determining zeolite content, utilizing an appropriate reference. Since the structure of the zeolite is known, the void volume and oxygen capacity can be calculated as a reference value. Nitrogen could be used but, because cation–nitrogen interactions would contribute to additional adsorption capacity, oxygen is preferred. A gravimetric microbalance of the McBain-Bakr type is used. Before adsorption, the zeolite sample is outgassed at 350–450°C under a reduced pressure of 1.3 mPa (10^{-5} mmHg) for 9–16 h. Complete isotherms should be measured in order to determine deviation from the type I contour. In the petroleum industry, hydrocarbons are frequently employed as adsorbates (69). These have the advantage that different-size molecules can distinguish between zeolites in a mixture, eg, high silica zeolites of type A topology and zeolite Y; *n*-hexane is sorbed by both zeolites, whereas only the latter sorbs cyclohexane.

9. Health and Safety Factors

Zeolites have applications in food, drugs, cosmetic products, and detergents. Thus, extensive toxicological and environmental studies have been carried out (70). In single oral-incubation studies, rats have survived a single massive dose equivalent to 32 g/kg of body weight (powder form of type 4A, 5A, 13X, and Y). Feeding of 5.0 g/kg of body weight for seven days produced no ill effect (71). There is no contraindication to the use of zeolite A (Sasil) in detergents.

No negative effect on biological wastewater treatment was found. In toxicity studies using algae, macroinvertebrates, and fish, zeolite A showed no evidence of acute toxicity to four species of freshwater fish. No mortality was found for either cold- or warm-water fish exposed to suspensions of 680 mg/L.

10. Uses

Some commercially available molecular-sieve products and related materials are shown in Table 7, classified according to the basic zeolite structure types. In most cases, the water content of the commercial product is $<1.5–2.5$ wt%; certain products, however, are sold as fully hydrated crystalline powders.

10.1. Adsorption. Since the 1960s, molecular-sieve adsorbents have become firmly established as a means of performing difficult separations, including gases from gases, liquids from liquids, and solutes from solutions (45). They are supplied as pellets, granules, or beads, and occasionally as powders. The adsorbents may be used once and discarded or, more commonly, may be regenerated and used for many cycles. They are generally stored in cylindrical vessels through which the stream to be treated is passed. For regeneration, two or more beds are usually employed with suitable valving, in order to obtain a continuous process. As a unit operation, adsorption (qv) is unique in several respects. In some cases, one separation is equivalent to hundreds of mass-transfer units. In others, the adsorbent allows the selective removal of one component from a mixture, based on molecular size differences, which would be nearly impossible to perform by any other means. In addition, contaminants can be removed from fluid streams to attain virtually undetectable impurity concentrations. Adsorbents are used in applications requiring a few grams to several tons.

Regenerative adsorption units can be operated by a thermal-swing cycle, pressure-swing cycle, displacement-purge cycle, or inert-purge cycle. Combinations of these are frequently employed.

10.2. Purification. Purification refers to separations, wherein the feed stream is upgraded by the removal of a few percent or even traces of a contaminant (Fig. 12). A heated purge gas is usually employed for this purpose.

10.3. Water. The dehydration of natural gas and air was the first of the gas-purification applications of molecular sieves. Because of their high adsorptive selectivity for water and high capacity at low water partial pressures, molecular sieves were an obvious choice for water removal from natural gas and air before cryogenic extraction of helium and cryogenic separation of oxygen, nitrogen, and the rare gases, respectively. Molecular-sieve dehydration is used in the cryogenic production of liquefied natural gas (LNG), for small-peak demand-type storage facilities and giant base-load facilities. In addition, molecular sieves have proved to be the most effective dehydration technique for the cryogenic recovery of ethane and heavier liquids from natural gas.

Molecular sieve utilization in new processes has increased in the dehydration of cracked gases in ethylene plants before low temperature fractionation for olefin production. The type 3A molecular sieve is size selective for water molecules and does not coadsorb the olefin molecules.

Table 7. **Commercial Molecular Sieve Products**[a,b]

Zeolite type	Designation	Cation	Effective pore diameter, Å	Vendors unit cell parameter[c], Å
A, KA	3A[d,e]	K	3	UOP
	Zeolum A-3[d,e]			TOSOH
	Sylosiv A3[e]			Grace Davison
A, NaA	4A[d,e]	Na	4	UOP
	Zeolum A-4[d,e]			TOSOH
	Valfor G100			PQ
	Sylosiv A3[e]			Grace Davison
A, CaA	5A	Ca	5	UOP
	Zeolum A-5[d,e]			TOSOH
X, NaX	13A[d,e]	Na	10	UOP
	Zeolum F-9[d,e]			TOSOH
	Sylosiv A10[e]			Grace Davison
Y, NaY	LZY-54[d]	Na	10	UOP (5.0); $a_0 = 24.68$
	HSZ-320NAA[d,e]			TOSOH (5.5); $a_0 = 24.64$
	CBV 100			PQ (5.2); $a_0 = 24.64$
Y, NH_4Y	LZY-64, -84[d]	NH_4	10	UOP (5.1, 5.9); $a_0 = 24.70, 24.57$
	CBV 300			PQ (5.2); $a_0 = 24.68$
Y, HY	LZY-74	H	10	UOP (5.2); $a_0 = 24.52$
	HZS-320HOA[d]			TOSOH (5.5); $a_0 = 24.50$
	HZS-330HSA[d]			TOSOH (6); $a_0 = 24.50$
	CBV 400, 500			PQ (5.1, 5.2); $a_0 = 24.50, 24.53$
Y, USY	LZ-10, -20	H, Al	10	UOP (5.5, 5.6); $a_0 = 24.30, 24.35$
	HSZ-330HUA[d]			TOSOH (5.6); $a_0 = 24.40$
	CBV 600			PQ (5.2); $a_0 = 24.33$
Y, dealuminate	LZ-210	H	10	UOP (6.5–18); a_0 varies
	HSZ-360,390HUA[d]			TOSOH(14,600); $a_0 = 24.30, 24.27$
	CBV 712-780			PQ (11.5–80); $a_0 = 24.33–24.24$
L	LZ-KL	K	8	UOP (6.3)
	HSZ-500KOA			TOSOH (6.2)
Mordenite, small-pore	AW-300	Na, mixed	4	UOP
Mordenite, large-pore	HSZ-610-640NAA	Na	7	TOSOH (12,15,20)
	CBV 10A			PQ (13)
	CBV 20, 30A	NH_4		PQ (20,35)
	LZM-5, -8	H		UOP (10.7,18)
	HSZ620, 640HOA			TOSOH (15,16)
Chabazite	AW-500	mixed	5	UOP
Ferrierite	HSZ-720KOA	K, Na	4	TOSOH (16.8)
ZSM-5	MFI, S-115	H	6	UOP (30–45, 180–400)
	HSZ-690HUA			TOSOH (>200)
	CBV 3020, 5020,			PQ (30,50,80,150)

Table 7. (*Continued*)

Zeolite type	Designation	Cation	Effective pore diameter, Å	Vendors unit cell parameter[c], Å
	8020, 1502			
Beta	CP 806B-25	Na, T[f]	7	PQ (25)
	CP 806BL-25	NH_4, T[f]		PQ (25)
	CP 811BL-25	H		PQ (25)
Zeolite F	Ionsiv F80	K, Na	4	UOP (2)
Zeolite W	Ionsiv W85	K, Na	4	UOP (3.6)

[a]Because of commercial usage, aringngstrom units (Å) are shown here. To convert to nm, divide by 10.
[b]All zeolite types are available as powders unless otherwise indicated. Chabazite and Mordenite, smallpore are available as extrudates only.
[c]For (SiO_2/Al_2O_3) by manufacturer indicated.
[d]Also available as extrudate.
[e]Also available as bead.
[f]T = template.

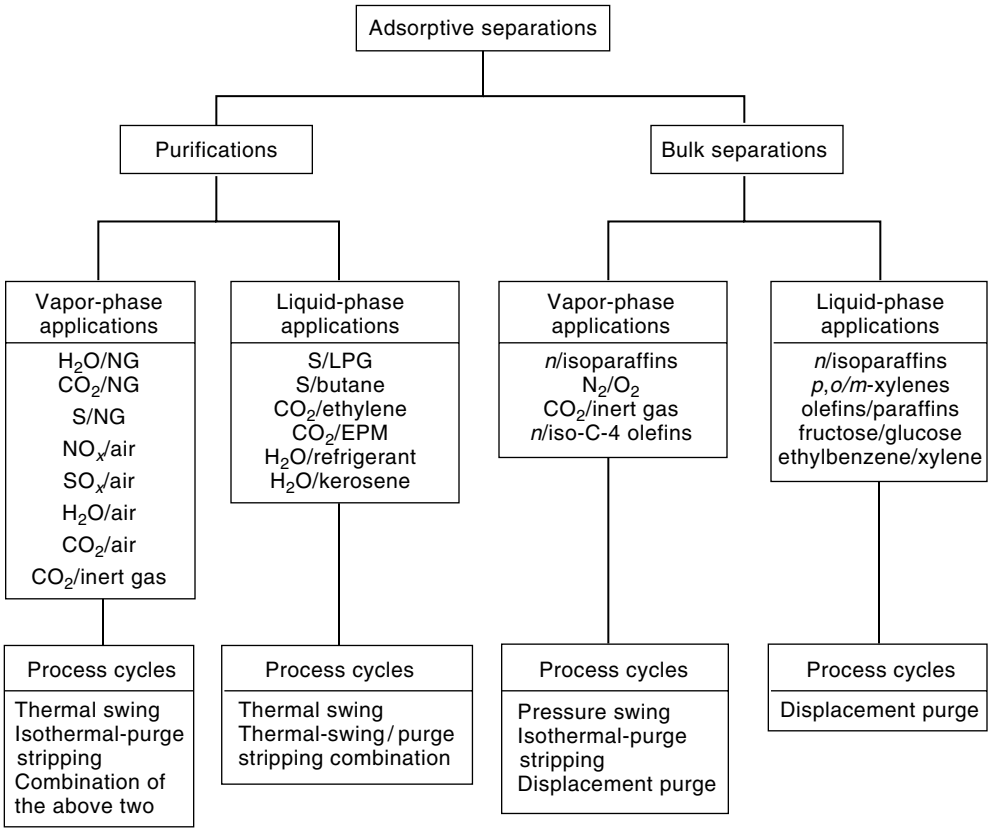

Fig. 12. Classification of adsorptive separations where NG = natural gas and S = sulfur.

The unique features of molecular sieves are demonstrated in the removal of water from natural gas streams containing high percentages of acid gases, eg, H_2S and CO_2. Other dry-bed adsorbents degrade in highly acidic environments. However, acid-resistant molecular sieves have been developed that maintain dehydration capacities over long periods of on-stream use. They also are used to dehydrate gas streams containing corrosive components such as chlorine, sulfur dioxide, and hydrogen chloride.

Molecular sieves are also used widely in the dehydration of liquid streams. Both batch-type and continuous processes have been developed for drying a variety of hydrocarbon and chemical liquids.

For nonregenerative drying, the molecular sieve is designed for the lifetime of the unit. A typical example is refrigerant drying and purification. A suitable-size cartridge of the proper molecular sieve, installed in the circulating refrigerant stream, adequately protects the refrigeration system from freeze-ups and corrosion for the life of the unit by adsorbing water and the acidic decomposition products of the refrigerant.

Another nonregenerative drying application for molecular sieves is their use as an adsorbent for water and solvent in dual-pane insulated glass windows. The molecular sieve is loaded into the spacer frame used to separate the panes. Once the window has been sealed, low hydrocarbon and water dew points are maintained within the enclosed space for the lifetime of the unit. Consequently, no condensation or fogging occurs within this space to cloud the window.

Gas and liquid dehydrators employing molecular sieves provide product gas streams of <0.1 ppmv water and product liquid streams routinely to <10 ppmv water. Applicable pressures range from <1 to several hundred times atmospheric pressure. Temperatures range from subzero to several hundred degree celcius. Processing units range in capacity from as little as $10\,m^3/h$ to as much as $10^8\,m^3/d$ in multiple-train units.

10.4. Carbon Dioxide. Molecular sieves are used to purify gas streams containing carbon dioxide in cryogenic applications where freeze-out of CO_2 would cause fouling of low temperature equipment. They are also employed for air purification in cryogenic air-separation plants where one front-end purifier unit can be used for the simultaneous removal of both water and CO_2. Peakshaving natural gas liquefaction is employed by utilities to store LNG during the summer. Molecular-sieve adsorbents remove water and CO_2 before liquefaction. Commercial processes are available for the removal of CO_2 from air, natural gas, ethylene, ethane–propane mix, and synthesis gases. Operations cover wide ranges of pressure and temperature.

10.5. Sulfur Compounds. Molecular sieves to remove sulfur contaminants treat various gas streams. In the desulfurization of wellhead natural gas, the unit is designed to remove sulfur compounds selectively, but not carbon dioxide, which would occur in liquid scrubbing processes. Molecular sieve treatment offers advantages over liquid scrubbing processes in reduced equipment size because the acid gas load is smaller; in production economics because there is no gas shrinkage (leaving CO_2 in the residue gas); and in the fact that the gas is also fully dehydrated, alleviating the need for downstream dehydration.

Molecular sieves are being used to treat refinery hydrogen streams containing trace amounts of H_2S. A single molecular sieve unit may be designed to

remove trace water and H_2S in the recycle hydrogen loop of a catalytic reformer to protect the catalyst from poisoning. Then, during catalyst regeneration, the same unit acts as a dryer for treating the inert gas used in regenerating the re-forming catalyst.

A large use of molecular sieves in the natural gas industry is LPG sweetening, in which H_2S and other sulfur compounds are removed. Sweetening and dehydration are combined in one unit and the problem associated with the disposal of caustic wastes from liquid treating systems is eliminated. The regeneration medium is typically natural gas. Commercial plants are processing from as little as $\sim 30\,m^3/d$ (200 bbl/day) to $>8000\,m^3/day$ (50,000 bbl/day).

10.6. Bulk Separation. The adsorptive separation of process streams into two or more main components is termed bulk separation (see Fig. 12). The development of processes and products is complex. Consequently, these processes are proprietary and are purchased as a complete package under licensing agreements. High purities and yields can be achieved.

Separation of Normal and Isoparaffins. The recovery of normal paraffins from mixed refinery streams was one of the first commercial applications of molecular sieves. Using type 5A molecular sieve, the *n*-paraffins can be adsorbed and the branched and cyclic hydrocarbons rejected. During the adsorption step, the effluent contains isoparaffins. During the desorption step, the *n*-paraffins are recovered. Isothermal operation is typical.

Regeneration is carried out by a pressure-swing process for a process separating light hydrocarbons (C-7). For heavier streams, a displacement-purge cycle employing lighter *n*-paraffins is used. The *n*-paraffins are separated by distillation from the regeneration effluent and recycled.

There are seven commercial processes in operation; six operate in the vapor phase. The Universal Oil Products process operates in the liquid phase and is unique in the simulation of a moving bed. The adsorption unit consists of one vessel segmented into sections with multiple inlet and outlet ports. Flow to the various segments is accomplished by means of a rotary valve that allows each bed segment to proceed sequentially through all the adsorption/desorption steps.

The normal paraffins produced are raw materials for the manufacture of biodegradable detergents, plasticizers, alcohols, and synthetic proteins. Removal of the *n*-paraffins upgrades gasoline by improving the octane rating.

Xylene Separation. *p*- Xylene is separated from mixed xylenes and ethylbenzene by means of the Parex process (Universal Oil Products Company). A proprietary adsorbent and process cycle are employed in a simulated moving-bed system. High purity *p*-xylene is produced.

Olefin Separation. Olefin-containing streams are separated either by the OlefinSiv process (Union Carbide Corp.) separating *n*-butenes from isobutenes in the vapor phase or the Olex process (Universal Oil Product) a liquid-phase process.

Oxygen from Air. A demand has developed for oxygen for processes needing from a few to ~50 t/day. In this size range, a pressure-swing adsorption process is often competitive with the conventional cryogenic separation route. Oxygen of 95% purity can be obtained; the main impurities are the inert gases found in air.

Catalysis. As of mid-2002, zeolite-based catalysts are employed in catalytic cracking, hydrocracking, isomerization of paraffins and substituted aromatics, disproportionation and alkylation of aromatics, dewaxing of distillate fuels and lube basestocks, and in a process for converting methanol to hydrocarbons (72).

Catalytic Cracking. The addition of relatively small amounts of hydrothermally stable acidic zeolites to conventional cracking catalyst formulations significantly increases both the yield and the quality of the products from fluidized- and moving-bed cracking reactors. At present, catalytic cracking is the largest scale industrial process employing zeolite catalysts. Catalysts containing the rare-earth-exchanged form or steam-stabilized forms of zeolite Y with or without rare-earth-exchange are marketed. The commercial catalysts comprise 5–40% zeolite dispersed in a matrix of synthetic silica–alumina, semisynthetic clay-derived gel, or natural clay. Such composites can be prepared either by blending a synthetic zeolite with a binder, or by chemical treatment of suitable clays to produce the zeolite component *in situ*.

Zeolite-promoted cracking catalysts offer the advantage of high rates of intermolecular hydrogen transfer coupled with extremely high intrinsic cracking activity, and the high thermal stability of the zeolite-cracking catalyst. Zeolite catalysts increase the yield of light cycle oil as well as the yield and octane of the gasoline product fraction, and decrease the production of coke and gas. The high cracking rates obtained with zeolite catalysts result in greatly reduced contact times for given conversion levels, thus further increasing liquid product yields. Additional advantages are increased tolerance to poisons and greater operating flexibility. The relationships between catalyst properties, feedstock composition, and reactor operating conditions are very complex (72). Additional incorporation of the shape-selective zeolite ZSM-5 in the cracking catalyst yields gasoline of improved octane rating (73).

In FCC, the major focus of current development is Short Contact Time (SCT) technology and a key element in the success of this technology is the catalyst. Akzo Nobel, Engelhard and Grace are the leading developers and suppliers of the SCT zeolite catalysts. The zeolite catalysts under go hydrothermal and chemical treatment for dealumination and ultrastablization to produce materials with mesopores and high surface area retention in the FCC unit, leading to improved activity and selectivity.

10.7. Hydrocracking for Fuels Production. Hydrocracking is catalytic cracking in the presence of hydrogen using a dual-function catalyst possessing both cracking and hydrogenation–dehydrogenation activity. At present, it is the second largest use for zeolite-containing catalysts. In general, such catalysts consist of an acidic, hydrothermally stable, large-pore zeolite loaded with a small amount of a noble metal, or admixed with a relatively large amount of an active hydrogenation system such as $NiO + MoO_3$ or WO_3.

Although several proprietary hydrocracking technologies are in use, the Union Oil Co. Unicracking process exemplifies the value of zeolite catalysts in broadening the range of feedstocks that can be handled and in simplifying hydrocracker design and operation. The most elaborate and versatile Unicracking process scheme is the two-stage configuration shown in Figure 13. Feedstock is mixed with hydrogen and admitted to reactor R-1, a conventional hydrotreater

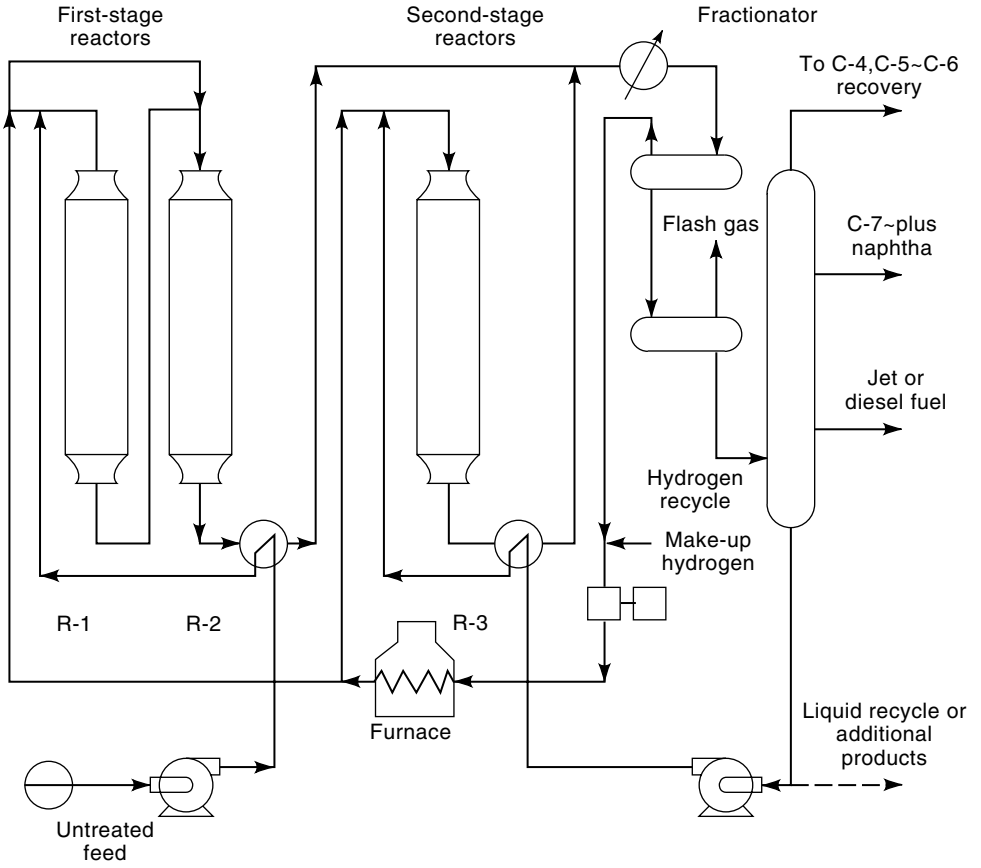

Fig. 13. Two-stage Unicracking unit (21). (Courtesy of American Chemical Society.)

in which it is substantially freed of nitrogen and sulfur compounds. The product then enters the first-stage Unicracker, R-2, in which it is hydrocracked, typically at a per-pass conversion of 40–70%. The zeolite catalysts developed for the Unicracking process can operate in a stable and efficient manner in the presence of hydrogen sulfide and ammonia. Thus, separation of these substances from the R-2 feed is not necessary. The fractionator bottoms are recycled through a second-stage reactor, R-3. The recycled gas that is mixed with the R-3 feed is essentially ammonia-free; thus the reactor can be operated efficiently at comparatively low temperatures and pressures while maintaining conversion at 50–80% per pass. In single-stage Unicracking, the R-2 product is treated in liquid–gas separators and fractionated.

In hydrocracking, as with all multipurpose refinery processes, the relationships between feedstock properties, catalyst-type, operating conditions, and product yield and character are complex. With zeolite catalysts, a variety of feedstocks is converted into a range of fuels, including LPG, medium-octane unleaded gasoline, and jet, diesel, and heating oils, or into feedstocks suitable for catalytic re-forming or petrochemical manufacture. Zeolite hydrocracking

catalysts are noted for permitting long (2–6 year) periods of highly efficient reactor operation at moderate conditions. Following such service, some of these catalysts can be completely restored to their original levels of activity.

10.8. Dewaxing of Distillate Fuels and Lube Basestocks. Removal of waxy molecules improves the cold-flow properties (pour point, freezing point, cloud point, and cold filter plugging point) of distillate fuels, which include jet and diesel fuels. The Mobil Distillate Dewaxing process, employing ZSM-5 catalyst, was commercialized in 1974 and is in use worldwide. Typical operating conditions are 260–430°C, 2–5.5 MPa (20–55 atm), 250–440-m^3 H_2/m^3 distillate (39). This process selectively cracks the waxy molecules, mainly consisting of straight-chain and methyl-substituted straight-chain hydrocarbons. Two-thirds of the cracked by-product is gasoline of sufficiently high octane rating, to be blended directly into the gasoline pool.

10.9. Paraffin Isomerization. Another well-established commercial process that employs zeolite catalysts is the isomerization of normal paraffins into higher octane, branched isomers. The catalyst for the Hysomer process of the Shell Oil Co. is dual-functional, and consists of a highly acidic, large-pore zeolite loaded with a small amount of a noble-metal hydrogenation component. This catalyst possesses the same hydrogenation–dehydrogenation and acid functions as hydrocracking catalysts. However, since hydrocracking of the Hysomer feedstock, which is usually a light, straight-run naphtha containing principally pentanes and hexanes, is not desired because it represents a direct reduction of gasoline yield, the process operating conditions are more stringently defined than those for hydrocracking. In general, reaction conditions are adjusted to allow the lowest possible reactor temperature consistent with economical production rates, since lower temperatures favor higher equilibrium concentrations of branched isomers, as well as the lowest hydrogen pressure consistent with economy of operation. In this way, yields of the highest octane highly branched isomers are maximized, and hydrocracking is minimized.

The Hysomer process produces an increase of ~12 octane numbers in suitable naphtha feedstocks. The process can be operated in conjunction with the Isosiv process (Union Carbide Corp.) for the separation of normal and isoparaffins, achieving complete isomerization of a C-5–C-6 stream. The combined process is trade named TIP (total isomerization process), and results in increases in octane numbers of ~20, rather than the 12 obtained with a once through Hysomer treatment.

10.10. Catalysis of Aromatic Reactions. In the 1960s, zeolite syntheses that included organic cations such as quaternary ammonium species in addition to the traditional alkali metal ions were developed, leading to a number of new molecular sieves. Mobil Corp. laboratories developed, among other zeolites, the zeolite ZSM-5. This zeolite is characterized by an unusual pore structure, the openings of which are 10-membered rings, and highly siliceous frameworks, with SiO_2:Al_2O_3 molar ratios of 20 to >10,000. The exceptional shape selectivity of ZSM-5 has been utilized to prepare some unique catalysts for a variety of processes (39).

10.11. Selective Toluene Disproportionation. The process entails toluene disproportionate over ZSM-5 to benzene and a mixture of xylenes. Unlike this reaction, over amorphous silica–alumina catalyst, ZSM-5 produces a xylene

mixture with increased *p*-isomer content compared with the thermodynamic equilibrium. Chemical modification of the zeolite crystal surface causing partial pore blockage produces catalysts that achieve almost 100% selectivity to *p*-xylene. This favorable result is explained by the greatly reduced diffusivity of *o*- and *m*-xylene compared with that of the less bulky *p*-isomer. For the same reason, large crystals (3 μm) of ZSM-5 produce a higher ratio of *p*- xylene than smaller crystallites (46,75).

10.12. Xylene Isomerization. The objective of C-8 aromatics processing is the conversion of the usual four-component feedstream (ethylbenzene and the three xylenes) into pure xylene isomers. Although the bulk of current demand is for *p*-xylene isomer for polyester fiber manufacture, significant markets for the other isomers exist. The primary problem is separation of the 8–40% ethylbenzene that is present in the usual feedstocks, a task that is complicated by the closeness of the boiling points of ethylbenzene and *p*-xylene. In addition, the equilibrium concentrations of the xylenes present in the isomer separation train raffinate have to be reestablished to maximize the yield of the desired isomer.

In the most readily adopted C-8 aromatics process based on ZSM-5 and related zeolites, the catalyst is an acid form of the sieve added optionally with a Groups 8–10 (Group VIII) metal to avoid hydrogenation of aromatic rings, among other goals (46). Such catalysts can be used in existing plants in place of the Pt/silica–alumina materials originally developed for the process. They have the advantages of higher throughput, owing to the ability to operate at low H_2/hydrocarbon ratios, and longer run life between regenerations. The shape-selectivity of the catalyst greatly favoring diffusion of the *p*-isomer permits higher than equilibrium concentrations of *p*-xylene to be produced. Transalkylation and dealkylation convert ethylbenzene present in the feedstock, yielding benzene of nitration-grade purity (28). ExxonMobil recently introduced XyMax for improved xylene isomerization in 2001, which increases ethylbenzene conversions upto 80% and futher reduces xylene losses by 50%.

10.13. Ethylbenzene Synthesis. The synthesis of ethylbenzene for styrene production is another process in which ZSM-5 catalysts are employed. Although some ethylbenzene is obtained directly from petroleum, ~90% is synthetic. In earlier processes, benzene was alkylated with high purity ethylene in liquid-phase slurry reactors with promoted $AlCl_3$ catalysts or the vapor-phase reaction of benzene with a dilute ethylene-containing feedstock with a BF_3 catalyst supported on alumina. Both of these catalysts are corrosive and their handling presents problems.

These operations have been gradually replaced by the ExxonMobil-Badger process (46), which employs an acidic ZSM-5 catalyst and produces ethylbenzene using both pure and dilute ethylene sources. In both cases, the alkylation is accomplished under vapor-phase conditions of ~425°C, 1.5–2 MPa (15–20 atm), 300–400-kg benzene/ kg catalyst/ h, and a benzene: ethylene feed ratio of ~30. ZSM-5 inhibits formation of polyalkylated benzenes produced with nonshape-selective catalysts. With both ethylene sources, raw material efficiency exceeds 99%, and heat recovery efficiency is high (see XYLENES AND ETHYLBENZENE).

10.14. Synthesis of Cumene. Several zeolite-based processes are available for cumene production. The advantages of the zeolite process over the older solid phosphoric acid (SPA) catalyst process is the excellent purity

and higher yield as well as the less corrosive and fewer catalyst disposal issues. Different zeolite/molecular sieves catalysts are used: ExxonMobil/Badger-Raytheon uses a proprietary zeolite MCM-22, UOP and Enichem uses large pore zeolite Beta and Dow/Kellogg Brown and Root technology is based on a 3D dealuminized mordenite (3-DDM).

10.15. Synthesis of *p*-Ethyltoluene. *para*-Ethyltoluene, the feedstock for *p*-methylstyrene, is difficult to separate from the products of toluene alkylation with ethane using conventional acidic catalysts. The unique configurational diffusion effect of ZSM-5 permits *p*-dialkylbenzenes to be produced in one step. In the alkylation of toluene with ethylene over a chemically modified ZSM-5, *p*-ethyltoluene is obtained at 97% purity (75).

10.16. The Methanol-to-Gasoline Process. Mobil Corp. laboratories have reported the conversion of methanol and some other oxygenated organic compounds to hydrocarbons using an acidic ZSM-5 zeolite catalyst (39). In the case of methanol, the highly exothermic reaction sequence includes the formation of dimethyl ether. The process is quite selective in producing an aromatics-rich gasoline-range mixture of hydrocarbons free of oxygen compounds. Several mechanisms have been proposed for this reaction, but none has been shown unequivocally to be correct (r39). The hydrocarbon product typically contains no compounds with >10 carbon atoms, and this, in conjunction with the lower than predicted concentrations of certain polyalkylated benzenes, is construed as evidence of shape selectivity owing to the moderate pore size of the catalyst. The process has been in commercial operation for many years in New Zealand, which has no crude oil deposits, and where methanol is produced from abundant natural gas. It is not competitive with the refining of crude oil.

A variation of this process is Mobil's methanol-to- olefins (MTO) process, in which up to 80% C_2–C_5 olefins are produced over ZSM-5 of reduced acidity and at much higher temperatures.

10.17. Ion Exchange. Crystalline molecular sieve ion exchangers do not follow the typical rules and patterns exhibited by organic and other inorganic ion exchangers. Many provide combinations of selectivity, capacity, and stability superior to the more common cation exchangers. Their commercial utilization has been based on these unique properties (76).

10.18. Cesium and Strontium Radioisotopes. Because of their stability in the presence of ionizing radiation and in aqueous solutions at high temperatures, molecular sieve ion exchangers offer significant advantages in the separation and purification of radioisotopes. Their low solubility over wide pH ranges, together with their rigid frameworks and dimensional stability and attrition resistance, have endowed zeolites with properties that generally surpass those of the other inorganic ion exchangers. The high selectivities and capacities of several zeolites for cesium and strontium radioisotopes resulted in the development of processes currently used by nuclear processing plants.

10.19. Ammonium Ion Removal. A fixed-bed molecular-sieve ion-exchange process has been commercialized for the removal of ammonium ions from secondary wastewater treatment effluents. This application takes advantage of the superior selectivity of molecular-sieve ion exchangers for ammonium ions. The first plants employed clinoptilolite as a potentially low cost material

because of its availability in natural deposits. The bed is regenerated with a lime-salt solution that can be reused after the ammonia is removed by pH adjustment and air stripping. The ammonia is subsequently removed from the air stream by acid scrubbing.

10.20. Detergent Builders. The prime function of phosphates in detergents is to reduce the activity of the hardness ions, Ca^{2+} and Mg^{2+}, in the wash water by complexing. Zeolite ion exchangers in powder form replace Ca^{2+} and Mg^{2+} in the solution with ions such as Na^{+}. Heavy-duty detergents employ the sodium form of type A zeolite for this purpose in low or zero-phosphate formulations. The zeolite powder is incorporated into the detergent powder during formulation. Large amounts of zeolite are used in this application.

11. New Trends

The foregoing discussion has focused on the most important commercial molecular sieves, zeolites. New directions in the preparation of framework structures of different chemical composition and of large-pore molecular sieves have also appeared and revolutionized the field of molecular sieve synthesis and potential applications of these classes of materials.

12. Mesoporous Molecular Sieves

A new family of molecular sieves with pore diameters in the mesoporous range ($\sim$2–50 nm) had been reported by the researchers at the Mobil Oil Corporation (11) opening a new chapter in molecular sieve technology. The designation given to this extensive family of ordered mesoporous molecular sieves is M41S. The extremely large surface area ($>1000\,m^2/g$) and the precise tuning of the pore sizes are among the many desirable properties that have made these materials the focus of many researchers around the world. The M41S materials initiated a novel approach in materials synthesis where, instead of using single molecules as templating agents, self-assembled molecular aggregates or supramolecular assemblies are employed as the structure-directing agents. The M41S family of materials was synthesized by the reaction of a silica source, an alkyltrimethylammonium surfactant, base and water. The mixture held at elevated temperature ($>100^{\circ}C$) for 24–200 h, affords a white solid, isolated by filteration or centriguation and calcined at 500°C to obtain the ordered mesoporous materials. The X-ray diffraction patterns of these materials are rather unique and consist of a strong low angle line with a *d*-spacing that correlates, but is not identical, with the pore diameter, and several higher order lines of lower intensity. Of particular interest are the three members of this family: MCM-41 (for Mobil Composition of Matter number 41), which possesses a hexagonal array of uniform mesopores, MCM-48, which is a cubic phase (space group Ia3d) and MCM-50, which is a lamellar phase (77).

A liquid-crystal templating mechanism was proposed by the Mobil researchers, based on the similarities between the liquid-crystalline surfactant assemblies (ie, lyotropic phases) and the M41S materials. The mesoporous

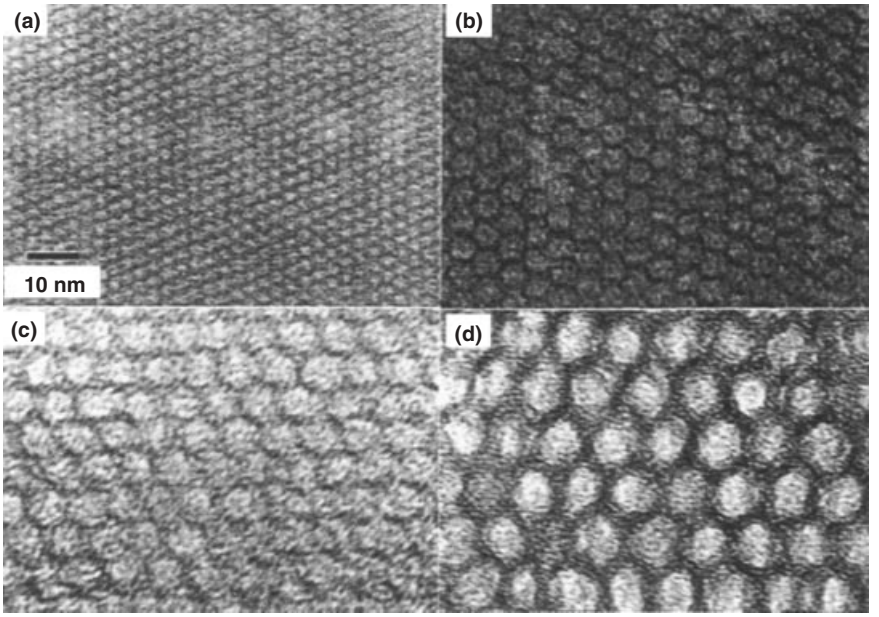

Fig. 14. Transmission electron micrographs of MCM-41 having pore diameters of (**a**) 2 nm, (**b**) 4 nm, (**c**) 6 nm, and (**d**) 8 nm (14).

structure dependence on the hydrocarbon chain length of the surfactant tail group, the effect of variation of surfactant concentrations and the influence of organic swelling agents (77) were the key features to support the hypothesis. The transmission electron microscopic images of the hexagonal MCM-41 family are shown in Figure 14, which clearly illustrates ability of fine tuning the pore sizes of these materials.

The crystallinity observed in the mesoporous materials is owed to the long-range ordering of the pore packing/stacking. The pore walls of these materials are amorphous and silanol groups cover the surface of the pores. Functionalization of the surface by the reaction of silylation reagents such as trimethylsilylchloride, with the silanols within the pore walls is just one of the examples for modification of these materials. Silylation of the pore walls not only can be effective method of reducing the pore diameter and pore volume but can also affect the hydrophilicity of the mesoporous material.

Functionalization the walls of the mesoporous materials with other organic moieties have expanded the area of immobilization of catalyst also termed as heterogenizing homogeneous catalysts, by anchoring organometallic compounds and metal sequestering ligands and chelants on the surface (78). Encapsulation and surface grafting afford confined nonagglomerized metal ligand species or nanoparticles. Systematic investigation have yield novel reaction pathways and products arising from sterically hindered active sites and some of these routes have surpassed the existing oragnometallic chemistries. Some interesting potential applications include adsorbents for toxic metal ions (79) and reactors for the production of high molecular weight crystalline polymers (80).

Over the past decade this field has expanded tremendously into new compositions and structural diversity, as well as in processability on the macroscale. A major thrust has been to stabilize various non-siliceous and transition metal oxides (81). The extention into the transition metal oxides lends these materials to have potential in not only catalysis but also in photonics, electronic and magenatic applications. The area has extended this basic motif of "liquid crystalline templating" to the point where it is possible to synthesize framework architectures with a numerous structural features and pore size regimes. This has lead to bridging the gap from the micro- to the macro size regime by employing not just self assembled surfactant phases, rather broadening the templating species to include amphiphilic block copolymers, vesicles, emulsion-stabilized oil droplets and even micron level latex spheres (82).

12.1. Macroporous Molecular Sieves. The remarkable 3D ordering of the latex particle templating to create macroporous materials (17) with pore/cage size of (~50–1000 nm) has extended the porous inorganic materials or molecular sieves materials to a new height. A simple and elegant process led by closed pack aggregation of the latex beads and then filling the interstitial spaces with a fluid precursor capable of solidification affords these remarkable materials. The removal of the template by chemical or thermal treatment produces a porous inverse replica of a macroporous material. Since the colloidal crystal templates consist of solid spheres in a closed packed array reminiscent of the opal structure, the macroporous product has been referred to as "inverse opal". The development of the new field has occurred very rapidly and the technique is amiable to a various synthetic routes to fill the tetrahedral and octaheral voids, routes such as sol–gel, salt solution, CVD, nano-crystalline and other precursors. This has led to a rich diversity in the chemical composition of the materials obtained from simple oxides, ternary oxides, metal chalcogens, metallic and non-metallic elements, alloys and polymers (83).

BIBLIOGRAPHY

"Molecular Sieves" in *ECT* 3rd ed., Vol. 15, pp. 638–669, by D. W. Breck and R. A. Anderson, Union Carbide Corp.; in 4th ed., Vol. 16, pp. 888–925, by Günter H. Kühl and Charles T. Kresge, Mobil Research and Development Corp.; "Molecular Sieves" in *ECT* (online), posting date: December 4, 2000 by Günter H. Kühl and Charles T. Kresge, Mobil Research and Development Corp.

CITED PUBLICATIONS

1. D. W. Breck, *Zeolite Molecular Sieves, Structure, Chemistry, and Use*, John Wiley & Sons, Inc., New York, 1974. H. van Bekkum, E. M. Flanigen, P. A. Jacobs, and J. C. Jansen, *Introduction to Zeolite science and Practice*, 2nd ed., *Stud. Surf. Sci. Catal.* Vol. **137**, Elsevier, 2001.
2. S. T. Wilson, B. M. Lok, C. A. Messina, T. R. Cannan, and E. M. Flanigen, *J. Am. Chem. Soc.* **104**, 1146 (1982); S. T. Wilson, B. M. Lok, C. A. Messina, and E. M. Flanigen, *ACS Symp. Ser.* **218**, 79 (1983).

3. B. M. Lok, C. A. Messina, R. L. Patton, R. T. Gajek, T. R. Cannan, and E. M. Flanigen, *J. Am. Chem. Soc.* **106**, 6092 (1984).
4. U.S. Pat. 4,554,143 (Nov. 19, 1985), C. A. Messina, B. M. Lok, and E. M. Flanigen (to Union Carbide Corporation); U.S. Pat. 4,567,029 (Jan. 28, 1986), S. T. Wilson and E. M. Flanigen (to Union Carbide Corporation); S. T. Wilson and E. M. Flanigen, *ACS Symp. Ser.* **398**, 329 (1989).
5. E. M. Flanigen, B. M. Lok, R. L. Patton, and S. T. Wilson, *Pure Appl. Chem.* **58**, 1351 (1986).
6. U.S. Pat. 4,880,761 (1989) R. L. Bedard, L. D. Vail, S. T. Wilson, E. M. Flanigen; *Stud. Surf. Sci. Catal.* **49A**, 375 (1989).
7. R. M. Dessau, J. L. Schlenker, and J. B. Higgins, *Zeolites* **10**, 522 (1990).
8. P. Wagner, M. Yoshikawa, M. Lovallo, K. Tsuji, M. Taspatsis, and M. E. Davis, *Chem. Commun.* 2179 (1997)
9. R. F. Lobo, M. Tsapatsis, C. C. Freyhardt, S. Khodabandeh, P. Wagner, C. Y. Chen, K. J. Balkus, S. I. Zones, and M. E. Davis, *J. Am. Chem. Soc.* **119**, 8474–8484 (1997).
10. A. K. Cheetham, H. Fjellvag, T. E. Gier, K. O. Kongshaug, K. P. Lillerud, and G. D. Stucky, *Stud. Surf. Sci. Catal.* **135**, 158 (2001); SSZ-53 and SSZ-59: A. Burton, S. Elomari, L. M. Bull, I. Y. Chan, C. Y. Chen, R. C. Medrud, C. Kibby, E. S. Vittoratos, and S. Zones, *Chem. Eur. J.* in press.
11. M. E. Davis, C. Montes, and J. M. Garces, *ACS Symp. Ser.* **398**, 291 (1989); ECR-34: K. G. Strohmaier, and D. E. W. Vaughan, D. E. W., *J. Am. Chem. Soc.* **125**, 16035 (2003).
12. J. Patarin, C. Schott, A. Merrouche, H. Kessler, M. Soulard, L. Delmotte, J. L. Guth, and J. F. Joly, *Proc. 9th Intern. Zeolite Conf. I* 263 (1993).
13. P. B. Moore and J. Shen, *Nature (London)* **306**, 356 (1983).
14. C. T. Kresge, M. E. Leonowicz, W. J. Roth, J. C. Vartuli and J. S. Beck, *Nature (London)* **359**, 710 (1992); J. S. Beck, J. C. Vartuli, W. J. Roth, M. E. Leonowicz, C. T. Kresge, K. D. Schmitt, C. T-W. Chu, D. H. Olson, E. W. Sheppard, S. B. McCullen, J. B. Higgins, and J. L. Schlenker, *J. Am. Chem. Soc.* **114**, 10834 (1992).
15. D. Zhao, J. Feng, Q. Huo, N. Melosh, G. H. Fredrickson, B. F. Chmelka, and G. D. Stucky, *Science* **279**, 548 (1998).
16. Q. Huo, D. I. Margolese, U. Ciesia, P. Feng, T. E. Gler, P. sieger, R. Leon, P. M. Petroff, F. Schuth and G. D. Stucky, *Nature (London)* **368**, 317 (1994).
17. B. T. Holland, C. F. Blanford, and A. Stein, *Science* **281**, 538 (1998); J. Wijnhoven and W. L. Vos, *Science* **281**, 802 (1998).
18. J. L. Schlenker and G. H. Kühl, *Proc. 9th Inter. Zeolite Conf. I* **3** (1993).
19. Ch. Baerlocher, W. M. Meier, and D. H. Olson, *Atlas of Zeolite Framework Types*, Elsevier Science B. V., 2001. Web page : www.iza-structure.org/databases/
20. L. B. Sand and F. A. Mumpton, eds., *Natural Zeolites, Occurrence, Properties, Use*, Pergamon Press, Oxford, U.K., 1978, pp. 135–350.
21. J. J. Pluth and J. V. Smith, *Amer. Mineral.* **75**, 501 (1990); J. V. Smith, J. J. Pluth, R. C. Boggs, and D. G. Howard, *J. Chem. Soc., Chem. Commun.* 363 (1991).
22. A. Alberti, G. Vezzalini, E. Galli and S. Quartieri, *Eur. J. Mineral.* **8**, 69 (1996).
23. E. Galli, G. Vezzalini, S. Quartieri, A. Alberti, and M. Franzini, *Am. Mineral.* **82**, 423 (1997).
24. E. Galli, G. Vezzalini, S. Quartieri, A. Alberti, and M. Franzini, *Zeolites.* **19**, 318 (1997).
25. L. Pauling, *Proc. Natl. Acad. Sci. U.S.A.* **16**, 453 (1930).
26. F. A. Mumpton, in L. B. Sand, and F. A. Mumpton, eds., *Natural Zeolites, Occurrence, Properties, Use*, Pergamon Press, New York, 1978, p. 3.

27. G. T. Kokotailo, S. L. Lawton, D. H. Olson, and W. M. Meier, *Nature (London)* **272**, 437 (1978).
28. E. M. Flanigen, J. M. Bennett, R. W. Grose, J. P. Cohen, R. L. Patton, R. M. Kirchner, and J. V. Smith, *Nature (London)* **271**, 512 (1978).
29. J. V. Smith, *ACS Monogr.* **171**, 3 (1976).
30. P. Wagner, O. Terasaki, S. Ritsch, J. G. Nery, S. I. Zones, M. E. Davis, and K. Hiraga, *J. Phys. Chem. B* **103**, 8245 (1999).
31. U.S. Pat. 6,049,018 (1999) D. C. Calabro, J. C. Cheng, R. A. Crane, C. T. Kresge, S. S. Dhingra, M. A. Steckel, D. L. Stern, and S. C. Weston.
32. M. J. Annen and M. E. Davis, *Chem Commun.* 1175 (1991); C. C. Freyhardt, R. F. Lobo, S. Khodabandeh, J. E. Lewis, Jr., M. Tsapatsis, M. Yoshikawa, M. A. Camblor, M. Pan, M. M. Helmkamp, S. I. Zones, and M. E. Davis, *J. Am. Chem. Soc.* **118**, 7299 (1996); L. B. McCusker, R. W. Grosse-Kunstleve, Ch. Baerlocher, M. Yoshikawa, and M. E. Davis, *Microporous Mater.* **6**, 295 (1996).
33. M. A. Camblor, A. Corma, P. Lightfoot, L. A. Villaescusa, and P. A. Wright, *Angew. Chem. Int. Ed. Engl.* **36**, 2659 (1997); L. A. Villaescusa, P. A. Barrett, and M. A. Camblor, *Chem. Commun.* 2329 (1998).
34. U.S. Pat. 6,471,939 (2002) T. Boix, M. Puche, M. A. Camblor, and A. Corma.
35. L. A. Villaescusa, P. A. Barrett, and M. A. Camblor, *Angew. Chem. Int. Ed. Engl.* **38**, 1997 (1999); A. Corma, M. T. Navarro, F. Rey, F. Rius, and S. Valencia, *Angew. Chem. Int. Ed. Engl.* **40**, 2277 (2001); A. Corma, M. J. Diaz-Cabanas, J. Martinez-Triguero, F. Rey, and J. Rius, *Nature (London)* **418**, 514 (2002); R. Castaneda, A. Corma, V. Fornes, F. Rey, and J. Rius, *J. Am. Chem. Soc.* **125**, 7820 (2003)
36. Q. Huo, R. Xu, S. Li, Z. Ma, J. M. Thomas, R. H. Jones, and A. M. Chippindale, *J. Chem. Soc., Chem. Commun.* 875 (1992).
37. T. E. Gier, and G. D. Stucky, *Nature (London)* **349**, 508 (1991).
38. X. H. Bu, P. Y. Feng, and G. D. Stucky, *Science* **278**, 2080 (1997).
39. N. Y. Chen, W. E. Garwood, and F. G. Dwyer, *Shape–Selective Catalysis in Industrial Applications*, Marcel Dekker, Inc., New York and Basel, 1989.
40. Ch. Baerlocher, W. M. Meier, and D. H. Olson, *Atlas of Zeolite Framework Types*, 5th rev. ed., Structure Commission of the International Zeolite Association, Elsevier, Amsterdam, The Netherlands, 2001.
41. R. M. Barrer, *Zeolites and Clay Minerals as Sorbents and Molecular Sieves*, Academic Press, London, 1978.
42. N. Y. Chen, *J. Phys. Chem.* **80**, 60 (1976).
43. P. A. Jacobs, *Carboniogenic Activity of Zeolites*, Elsevier Science Publishing Co., Inc., New York, 1977.
44. J. B. Uytterhoeven, *Acta Phys. Chem.* **24**, 53 (1978).
45. R. A. Anderson, *ACS Symp. Ser.* **40**, 637 (1977).
46. D. H. Olson, and W. O. Haag, *ACS Symp. Ser.* **248**, 275 (1984).
47. G. T. Kerr, *J. Catal.* **15**, 200 (1969); G. H. Kühl, *J. Phys. Chem. Solids* **38**, 1259 (1977).
48. G. T. Kerr, A. W. Chester, and D. H. Olson, *Acta Phys. Chem.* **24**, 169 (1978).
49. R. M. Dessau, *J. Catal.* **89**, 520 (1984).
50. U. Lohse, H. Stach, H. Thamm, W. Schirmer, A. A. Isirikyan, N. I. Regent, and M. M. Dubinin, *Z. Anorg. Allg. Chem.* **460**, 179 (1980).
51. J. Scherzer, *J. Catal.* **54**, 285 (1978).
52. H. K. Beyer, I. M. Belenykaja, F. Hange, M. Tielen, P. J. Grobet, and P. A. Jacobs, *J. Chem. Soc., Faraday Trans. I* **81**, 2889 (1985).
53. G. W. Skeels and D. W. Breck, in D. H. Olson and A. Bisio, eds., *Proceeding of the 6th International Zeolite Conference, Reno, Nev.*, Butterworths, Guildford, U.K., 1984, p. 87.

54. R. M. Dessau, and G. T. Kerr, *Zeolites* **4**, 315 (1984).
55. C. D. Chang, C.T. W. Chu, J. N. Miale, R. F. Bridger, and R. B. Calvert, *J. Am. Chem. Soc.* **106**, 8143 (1984).
56. D. S. Shihabi, W. E. Garwood, P. Chu, J. N. Miale, R. M. Lago, C. T. W. Chu, C. D. Chang, *J. Catal.* **93**, 471 (1985).
57. A. W. Chester, Y. F. Chu, R. M. Dessau, G. T. Kerr, and C. T. Kresge, *J. Chem. Soc., Chem. Commun.* 289 (1985).
58. R. M. Barrer, and B. Coughlin, *Molecular Sieves*, Society of Chemical Industry, London, 1968, p. 141.
59. K. Yamagishi, S. Namba and T. Yahima, *Bull. Chem. Soc. Jpn.* **64**, 949 (1991).
60. S. Han, K. D. Schmitt, D. S. Shihabi and C. D. Chang, *J. Chem. Soc., Chem. Commun.* 1287 (1993).
61. L. D. Rollmann, *Adv. Chem. Ser.* **173**, 387 (1979).
62. E. M. Flanigen, *Adv. Chem. Ser.* **121**, 119 (1973); S. P. Zhdanov, *Adv. Chem. Ser.* **101**, 20 (1971); F. G. Dwyer, P. H. Schipper, and F. Gorra, *Nat. Petr. Ref. Assoc.*, AM-87–63 (Mar. 1987); C. L. Angell and W. H. Flank, *ACS Symp. Ser.* **40**, 194 (1977).
63. G. T. Kerr, *J. Phys. Chem.* **70**, 1047 (1966).
64. G. T. Kerr, *J. Phys. Chem.* **72**, 1385 (1968).
65. Th. L. M. Maesen and B. Marcus, *Stud. Surf. Sci. Catal.* **137**, 1 (2001).
66. J. Lacson, S. Schlag, and A. Kishi, *Zeolites*, Marketing Research Report, *Chemical Economics Handbook*, SRI International, 599.1000A, 2002.
67. A. P. Bolton, in R. B. Anderson and P. T. Dawson, eds., *Experimental Methods in Catalysis Research*, Vol. **2**, Academic Press, Inc., New York, 1976, p. 1.
68. G. Engelhardt and D. Michel, *High-Resolution Solid-State NMR of Silicates and Zeolites*, John Wiley & Sons, Inc., New York, 1987.
69. G. R. Landolt, *Anal. Chem.* **43**, 613 (1973).
70. P. Berth, *J. Am. Oil Chem. Soc.* **55**, 52 (1978).
71. *Adsorbent Data Sheets, Nos. 3797, 4172, 4174, and 4175*, Union Carbide Corp., New York.
72. P. B. Venuto, and E. T. Habib, Jr., *Fluid Catalytic Cracking with Zeolite Catalysts*, Marcel Dekker, Inc., New York, 1979; T. F. Degnan, C. M. Morris, and C. R. Venkat, *Appl. Cat. A* **221**, 283 (2001); T. F. Degnan, *J. Catal.* **216**, 32 (2003) reference therein.
73. C. D. Anderson, F. G. Dwyer, G. Koch, and P. Niitranen, *Proceedings of the 9th Iberoamerican Conf. on Catalysis*, Lisbon (1984). T. F. Degnan, G. K. Chitnis, and P. H. Schipper, *Micropor. Mesopor. Mater.* **35**, 245 (2000).
74. N. Y. Chen, W. W. Kaeding, and F. G. Dwyer, *J. Am. Chem. Soc.* **101**, 6783 (1979).
75. W. W. Kaeding, L. B. Young, and A. G. Prapas, *Chemtech.* **12**, 556 (1982).
76. J. D. Sherman, *A. I. Ch. E. Symp. Ser.* **179**, 74, 98 (1978).
77. J. C. Vartuli, W. J. Roth, J. S. Beck, S. B. McCullen, and C. T. Kresge, *Molecular Sieves, Vol 1, Synthesis* H. G. Karge, and J. Weitkamp, eds., Springer-Verlag, Berlin Heidelberg, 1998).
78. A. Stein, B. J. Melde, and R. C. Schroden, *Adv. Mater.* **12**, 1403 (2000); A. Ayari, and S. Hamoudi, *Chem. Mater.* **13**, 3151 (2001); R. Anwander, *Chem. Mater.* **13**, 4419 (2001); A. P. Wight, and M. E. Davis, *Chem. Rev.* **102**, 3589 (2002); D. E. DeVos, M. Dams, B. F. Sels, and P. A. Jacobs, *Chem. Rev.* **102**, 3615 (2002).
79. X. Feng, G. E. Fryxell, L.-Q. Wang, A. Y. Kim, J. Liu, and K. M. Kemner, *Science* **276**, 923 (1997).
80. K. Kageyama, J. Tamazawa, and T. Aida, *Science* **285**, 2113 (1999).
81. F. Schuth, *Chem. Mater.* **13**, 3184 (2001); X. He and D Antonelli, *Angew. Chem. Int. Ed.* **41**, 214 (2002).

82. G. A. Soler-Illia, C. Sanchez, B. Lebeau, and J. Patarin, *Chem. Rev.* **102**, 4093 (2002).
83. A. Stein, *Microporous Mater.* **44–45**, 227 (2001).

GENERAL REFERENCE

J. A. Rabo, R. D. Bezman, and M. L. Poutsma, *Acta Phys. Chem.* **24**(1–2), 39 (1978).

CHARLES T. KRESGE
SANDEEP S. DHINGRA
The Dow Chemical Company